Aus der II. Medizinischen Klinik der Medizinischen Fakultät Mannheim
(Direktor: Prof. Dr. med. Matthias P. A. Ebert)

Bone Morphogenetic Protein (BMP)-9 acts tumour-suppressive by enhancing the ID1/Noggin ratio in colorectal cancer

Inauguraldissertation
zur Erlangung des medizinischen Doktorgrades
der
Medizinischen Fakultät Mannheim
der Ruprecht-Karls-Universität Heidelberg
zu
Heidelberg

vorgelegt von
Chen Cai

aus
Jiangsu
Volksrepublik China
2023

Dekan: Prof. Dr. med. Sergij Goerdt

Referentin: PD Dr. rer. nat. Katja Breitkopf-Heinlein

Table of Contents

1. List of Tables

2. List of Figures

3. Supplement

Suppl. Fig. 1: Intestinal crypts and villi.

Suppl. Fig. 2: Schematic presentation of organoids isolation.

Suppl. Fig. 3: RT-PCR of colorectal tumour Organoids cultured in different medium.

Suppl. Fig. 4: Expression levels of differentiation- and cell-type-markers in Tumor and Normal Organoids (T-Orgs and N-Orgs, respectively).

Suppl. Fig. 5: Analysis of the consensus molecular subtypes (CMS) of organoids from patients 082, 080 and 090.

Suppl. Fig. 6: Analysis of the mutation status of the tumours.

Suppl. Fig. 7: Analysis of the CMS subgroup of TP53 mutated patient's data

Suppl. Fig. 8: Enriched gene sets in T-Orgs compared to N-Orgs of all 3 patients.

Suppl. Fig. 9: Individual expression changes in T-Orgs compared to corresponding N-Orgs.

Suppl. Fig. 10: Noggin reduces and BMP-9 enhances ID1 expression in Organoids.

Suppl. fig. 11: BMP-receptor expression is not significantly changed in CAFs by co-culture with T-Orgs.

Suppl. Fig 12: Expression of Alk1 is mainly unchanged by co-culture in CAFs as well as T-Orgs.

4. Abbreviations

3D	3 dimensional
AC	adenocarcinoma
ACG	American College of Gastroenterology
ACR	American College of Radiology
ACS	Advanced Chelation Solution
ACS	American Cancer Society
bHLH	basic helix-loop-helix
BMI	Body Mass Index
CAFs	Cancer associated fibroblasts
CMS	consensus molecular subtypes
COAD	colon adenocarcinoma
CRC	Colorectal cancer
CTC	Computed Tomography Colonography
CT values	Cycle Threshold values
DEGs	differential expressed genes
DKFZ	Deutsches Krebs Forschungszentrum
DMSO	Dimethyl sulfoxide
DNA	Deoxyribonucleic acid
cDNA	complementary DNA
EDTA	Ethylendiamintetraacetat acid
EGF	epidermal growth factor
EMT	epithelial mesenchymal transition
FDR	False Discovery Rate
FIT	Fecal Immunochemical Test
FIT-DNA	Stool DNA
GENT	Gene Expression database of Normal and Tumor tissues
GEP	Gene Expression Profiles
GEPIA	Gene Expression Profiling Interactive Analysis
gFOBT	guaiac fecal occult blood test
GSEA	Gene Set Enrichment Analysis
HCC	hepatocellular carcinoma
HKG	Housekeeping genes

IF	immunofluorescent
KEGG	Kyoto Encyclopedia of Genes and Genomes
KO	knock-out
LogFC	log2 Foldchange
MAC	mucinous adenocarcinoma
MsigDB	molecular signatures database
NAFLD	non-alcoholic fatty liver disease
NCCN	National Comprehensive Cancer Network
NES	normalized enrichment score
OS	overall survival
PCR	polymerase chain reaction
q-PCR	quantitative real time polymerase chain reaction
RT-PCR	Reverse transcription polymerase chain reaction
PPI	Protein-Protein-Interaction
READ	rectum adenocarcinoma
RIN	RNA integrity number
RMA	Robust Multiarray Average
RNA	ribonucleic acid
mRNA	messenger RNA
SEM	standard error of the mean
SHH	sonic hedgehog
SRCC	signet ring cell carcinoma
STRING	Search Tool for the Retrieval of Interacting Genes/Proteins
T2DM	Type 2 diabetes mellitus
TA	transit amplifying zone
TCGA	The Cancer Genome Atlas
TME	tumour microenvironment
UICC	union for international cancer control
USMSTF	U.S. Multi-Society Task Force
USPSTF	U.S. Preventive Services Task Force
WT	wild type

Medium/ Buffer

DMEM	Dulbecco's Modified Eagle Medium
ENA	Medium for tumour Organoids, main factors: EGF, Noggin, A83-01
FCS	fetal calf serum
PBS	Phosphate-buffered saline
WENRA	Medium for normal Organoids, main factors: Wnt-3A and R-Spondin

Cells

HSC	hepatic stellate cells
aHSC	activated hepatic stellate cells
qHSC	quiescent hepatic stellate cells
HUVEC	human umbilical vein endothelial cells
LSEC	liver sinusoidal endothelial cells

Organoids

Orgs	Organoid(s)
N-Orgs	Normal Organoids
T-Orgs	Tumour Organoids

Mouse strain

129/Ola	mouse strain
BMP-9 KO mice	BMP-9 Knock Out mice
C57BL/6	mouse strain

Stem cells

ASC	adult stem cell
ESC	embryonic stem cell
PSC	pluripotent stem cell
iPSC	Induced pluripotent stem cell
MSC	mesenchymal stem cell

Gene/Protein	
ActR-II/ ACVR2A	activin A receptor type 2A
ActR-IIB/ ACVR2B	activin A receptor type 2B
ACVR1	activin A receptor type 1
ACVR2A	activin A receptor type 2A
ACVR2B	activin A receptor type 2B
ACVRL1	activin A receptor like type 1
ALK1	activin-like kinase receptor 1
ALK2	activin-like kinase receptor 2
AMHR-II	anti-Mullerian hormone receptor type 2
APC	APC regulator of WNT signaling pathway
b2M	beta-2-microglobulin
BAX	BCL2 associated X, apoptosis regulator
Bcl2	BCL2 apoptosis regulator
BMP	bone morphogenetic protein
BMP-2	Bone Morphogenetic Protein 2
BMP-4	Bone Morphogenetic Protein 4
BMP-5	Bone Morphogenetic Protein 5
BMP-6	Bone Morphogenetic Protein 6
BMP-7	Bone Morphogenetic Protein 7
BMP-9	Bone Morphogenetic Protein 9
BMP-13	Bone Morphogenetic Protein 13
BMP-14	Bone Morphogenetic Protein 14
BMPR-II	bone morphogenetic protein receptor type 2
BMPR1A	bone morphogenetic protein receptor type 1A
BMPR1B	bone morphogenetic protein receptor type 1B
BMPR2	bone morphogenetic protein receptor type 2
CA1	carbonic anhydrase 1
CCl2	C-C motif chemokine ligand 2
CDKN1A	cyclin dependent kinase inhibitor 1A
CXCL6	C-X-C motif chemokine ligand 6
CXCL8	C-X-C motif chemokine ligand 8
ENG	Endoglin

FABP	fatty acid binding protein
GDF2	Growth and Differentiation Factor 2
HGF	hepatocyte growth factor
HIF-1α	hypoxia inducible factor 1 subunit alpha
ID1	inhibitor of DNA binding 1
ID2	inhibitor of DNA binding 2
ID3	inhibitor of DNA binding 3
ID4	inhibitor of DNA binding 4
IL-6	interleukin 6
LGR5	leucine rich repeat containing G protein-coupled receptor 5
MHC	major histocompatibility complex, class I, C
MKI67	marker of proliferation Ki-67
Myc	MYC proto-oncogene, bHLH transcription factor
NOG	noggin
P-Smad1	phosphorylated SMAD1
PCNA	proliferating cell nuclear antigen
PTPRO	Protein tyrosine phosphatase, receptor type O
ROR gamma gene	RORC RAR related orphan receptor C
rS18	RS18, ribosomal protein 18 40S small ribosomal subunit
SLCA5	Solute Carrier Family 5 Member
SMAD1	SMAD family member 1
SMAD4	SMAD family member 4
SMAD5	SMAD family member 5
SMAD8	SMAD family member 8
SMAD9	SMAD family member 9
TGF-β	transforming growth factor beta
TGFβR-II	transforming growth factor beta receptor 2
TP53	tumor protein p53
VEGFA	vascular endothelial growth factor A
Wnt3A	Wnt family member 3A

Chemotherapy

FOLFOX	folinic acid, fluorouracil, oxaliplatin

FOLFIRI	folinic acid, fluorouracil, irinotecan
FOLFOXIRI	folinic acid, fluorouracil, oxaliplatin, irinotecan
XELOX	Capecitabine, oxaliplatin

5. Introduction

5.1 Colorectal cancer and therapy

5.1.1 Epidemiology and aetiology

Colorectal cancer (CRC) is still a leading cause of cancer-associated mortality worldwide[1]. In Germany alone, there are around 60.000 newly diagnosed CRC cases every year, of which half are rectum cancer[2]. Obesity, red meat or high-fat, low-fiber nutrition are known risk factors for colorectal cancer[3]. Moreover, genetic factors and precancerous lesions are also common causes of colorectal cancer[4], which makes exercise, low-fat and high-fiber diet as well as screening programs for people above 50 years very meaningful. Recommendations and clinical practice guidelines for colorectal screening were established by different organizations, in which guaiac fecal occult blood test (gFOBT), flexible sigmoidoscopy, coloscopy and computed tomography colonography are the most frequently used screening methods (table 1)[5] . Colonoscopy screening for example, in the group of 45-49 years of age is meaningful to detect potential early onset CRC patients, but because of the high costs, specifically targeted methods may be more suitable[6].

5.1.2 Physiopathology of colorectal cancer

The wall of the large intestine consists of the mucosa, submucosa, muscularis and serosa. The mucosa in turn consists of the epithelium, the lamina propria and the muscularis mucosae. Colonic crypts are test tube shaped like structures which are composed of epithelial cells[7]. The average perimeter of crypts is 23 cells[8] and the average cell number per crypt is around 1500-5000[9]. 5 to 6 stem cells whose cell surface marker is LGR5, stay at the bottom of the crypts and possess the feature of own replication, self-maintenance and multilineage differentiation ability (Suppl. Fig 1). Stem cell behaviour is affected by the stem cell niche, which is composed of basement membrane proteins and cells like myofibroblasts. The Wnt signaling pathway which promotes stem cell self-renewal and the BMP pathway that negatively regulates crypt cell proliferation are involved in the intestinal stem cell niche regulation[10].

Uncontrolled crypts cell division leads to adenomatous polyps or colorectal cancer[11]. Depending on the aberrant cell type, three major histological subtypes can be found in colorectal cancer: adenocarcinoma (AC), signet ring cell carcinoma (SRCC) and mucinous AC (MAC). These subtypes predict different patient overall survival (OS) in later stages of the disease[12]. Chromosomal instability, microsatellite instability and CpG island methylator phenotype pathways are the three identified pathways for molecular pathology of Colorectal cancer[13, 14].

5.1.3 Current Colorectal cancer therapy

Surgical treatment or tumour resection through Endoscopy are still the main therapy for colon cancer without metastases. Adjuvant Chemotherapy is recommended by the Union for international cancer control (UICC) for above stage II cancers. For patients who already developed metastases and obtained removal of as much tumour as possible but are otherwise still in good condition, chemotherapy like FOLFOX, FOLFIRI, FOLFOXIRI or XELOX is recommended. When patients already have metastases also palliative therapy which aims at alleviation of symptoms, or help in organization of nursing and social services as well as assistance and emotional support should be applied[15]. The 10-year survival rate after acute dissection in Germany is around 30-60%[16].

5.2 BMP-9 signaling

5.2.1 BMP-9 and its functions

Bone Morphogenetic Protein (BMP)-9, also called Growth and Differentiation Factor (GDF)-2, was first studied in osteogenesis and chondrogenesis[17 18]. Through combination with Type 1 receptors (activin-like kinase receptor 1, 2(ALK1, 2)) or type II receptors (ActR-II, ActR-IIB, BMPR-II, TGFβR-II, and AMHR-II) BMP9 can activate SMAD1/5/8, the latter then move into nucleus and activate target genes like ID1. However, a number of studies have additionally shown its functions in diverse

diseases such as obesity, diabetes[19], lung infections [20], acute respiratory distress syndrome[21], liver fibrosis[22, 23] and solid organ carcinoma[24-26]. BMP-9 seems to be important for liver disease development in non-alcoholic fatty liver disease (NAFLD), liver fibrosis and hepatocellular carcinoma (HCC) (Fig. 1) [27]. However, there were studies that also exhibited controversial roles of BMP-9 as being both anti- or pro-fibrogenic and also anti- or pro-tumourigenic[28, 29]. Specifically, BMP-9 KO mice that were generated in the 129/Ola mouse strain, showed dilated and capillarized hepatic sinusoids and spontaneously developed liver fibrosis[22]. Results from our group showed that BMP-9 is mainly expressed by hepatic stellate cells (HSC) in liver and that it has pro-fibrogenic effects in murine models of chronic liver injury[30]. On the other hand, the known role of BMP-9 in HCC also shows to be controversial as it can be pro-tumourigenic through the induction of HIF-1α/VEGFA[24] and anti-tumourigenic by inducing p21 signaling and cell cycle arrest[25].

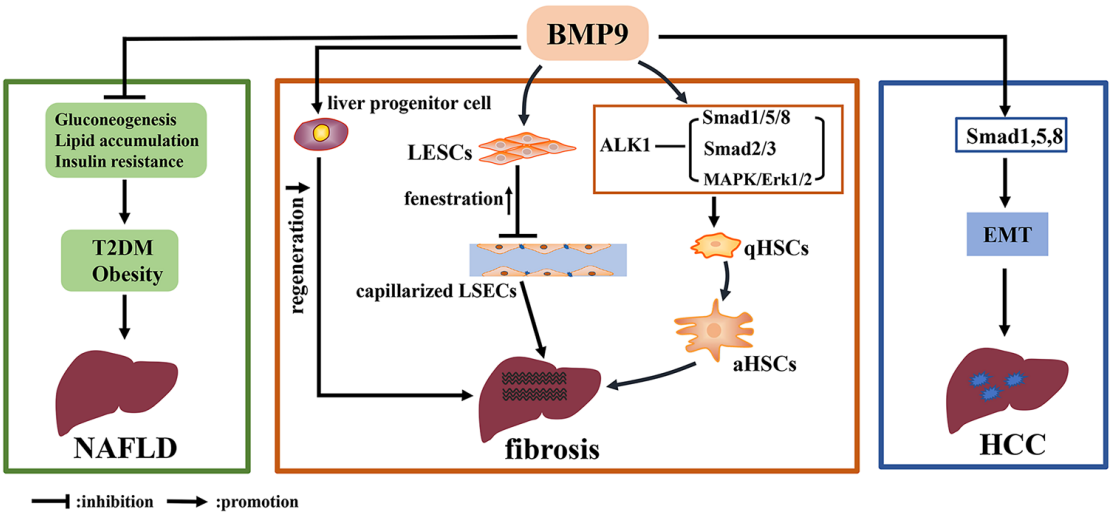

Fig. 1: **Schematic Illustration of the BMP9 effects on NAFLD, liver fibrosis and HCC.** T2DM: type 2 diabetes mellitus, LSECs: liver sinusoidal endothelial cells, EMT: epithelial mesenchymal transition, HSCs: hepatic stellate cells, qHSCs: quiescent HSCs, aHSCs: activated HSCs[27].

5.2.2 ID1 and its function

Inhibitor of DNA-binding protein 1 (ID1) is a protein that inhibits the DNA binding of transcription factors belonging to the group of basic helix-loop-helix (bHLH) proteins

which leads to inactivation of transcription. There are until now four IDs (ID1-ID4) described in humans, that are found in both nucleus und cytoplasm[31], having a half-live of less than one hour before they are being degraded[32]. ID proteins are important in cell cycle regulation, invasiveness, metastasis, chemoresistance, immune processes, bone formation, myogenesis, angiogenesis and they can initiate stemness[33]. They were also found to be up-regulated in different tumours and often play a pro-tumorigenic role[34, 35]. Rarely there are also reports about anti-tumorigenic functions of ID1. One study showed that ID1 induces apoptosis of developing thymocytes via E protein-dependent ROR gamma gene expression in ID1 transgenic mice[36]. ID1 is one of the main target genes of the BMP signalling pathway and BMP-9 induces it through activation of the Smad1/Smad5/Smad8 pathway[29, 37, 38].

5.2.3 Noggin and its function

Noggin is a glycosylated, secreted protein encoded by the NOG gene. Through combining and cut the binding between ligand and receptor sites of both types of receptors (Type I and Type II), Noggin can inhibit the functions of many BMPs including BMP2, 4, 5, 6, 7, 13 and 14 and it plays an important role in cell survival, proliferation and differentiation[39]. By blocking BMP-6, Noggin enhanced stem cell numbers in hippocampal tissue which could be a new therapeutic strategy for neuro-degenerative diseases[40]. By blocking BMP-2 Noggin prevents cartilage degeneration[41] and Noggin also supports angiogenesis in human umbilical vein endothelial cells (HUVECs) after down-regulation of BMP-4[42]. Recently, Sawant et al. reported that in the group of patients with a body mass index (BMI)>27 the expression levels of Noggin are clearly higher as compared to those with a BMI<27. Furthermore, together with Noggin certain transcription factors were increased that are essential for adipocyte differentiation, demonstrating a new function of Noggin in adipogenesis[43]. There exists so far, no direct research regarding Noggin and CRC, however, Noggin was found to be a poor prognostic factor for gastric cancer[44].

5.3 Organoids and CAFs

5.3.1 Three dimensional (3D) Organoids

Embryonic, adult or pluripotent stem cells (ESC, ASC or PSC) were isolated from tissue and cultured in matrigel in specific stem cell niche factors. Using their self-renewal and differentiation abilities they can form 3D, organ like structures, called Organoids. Organoids were first described by Smith and Cochrande in 1946 as "cystic Organoids teratoma"[45]. Since then, Organoids of different organs like colon[46], pancreas[47], liver[48] or brain[49] were developed and are nowadays being widely used in translational as well as basic research (Suppl. Fig 2)[50]. The advantage of Organoids is that this model can better mimic the tissue architecture and functionality of the in vivo situation, especially when Organoids are co-cultured with other cell types like fibroblasts. One disadvantage is that cell isolation and culture of Organoids is a time- and resource-consuming method.

5.3.2 Gut Organoids

Intestinal crypt-villus structured Organoids were first generated from Lgr5+ stem cells by Sato. et al in 2009[51]. The same group later established long-term culture protocols for Organoids from colonic epithelium, colonic adenocarcinoma and Barrett's esophagus[46]. While activation of classic WNT and Notch pathways and inhibition of BMP signaling are required for intestinal stemness, the WNT activator R-Spondin and Wnt3A together with the BMP antagonists Noggin are main parts of the intestinal/colon Organoids culture medium[46, 52].

5.3.3 CAFs

Cancer associated fibroblasts (CAFs) are important parts of the tumour microenvironment (TME)[53]. They secrete cytokines and chemokines, which play an important role in tumour proliferation, angiogenesis, metabolism, metastasis, therapy resistance and immune exclusion[54-56]. However, because of their heterogeneity, CAFs have not only tumour-promoting, but also potential tumour-restraining functions, as immunosuppression[57] and inhibition or genetic deletion of sonic hedgehog (SHH) in CAFs led to decreased survival[58]. Unfortunately, there are no specific CAFs subgroup

markers to further clarify the opposite functions of different subgroups. Several precursors of CAFs though were suggested: mesenchymal stem cells (MSCs), pancreatic and hepatic stellate cells, resident fibroblasts, or even other non-fibroblastic, well differentiated cell types like adipocytes, endothelial cells, pericytes and epithelial cells[58].

5.4 Aims

The main aims of this study were:

- To optimize the experimental setup using gut Organoids: The widely used organoid-media (ENA and WENRA) contain many factors and inhibitors like e.g. Wnt, R-Spondin, EGF or Noggin (see complete list in table 3) which could affect or interfere with BMP-9 signalling. Therefore the first aim was to test reduced media-recipes and to finally demonstrate that such basal medium containing profoundly less factors, is still suitable for our experiments and does not alter the Organoids morphology, viability, functionality and differentiation-state.
- Secondly, we wanted to characterize the Organoids that were generated from primary human tissue in terms of cellular composition and comparability to the in vivo situation (tumour- as well as normal tissue).
- Thirdly, we wanted to analyse the possible role of BMP-9 in colorectal cancer. For this aim in silico data obtained from human colorectal patient material should be analysed and Organoids should be studied in vitro upon stimulation with BMP-9 and/or Noggin. Finally, possible BMP-9 target cells should be identified using samples from BMP-9 knockout mice.
- Lastly, a co-culture setup to study the interaction of Organoids and CAFs should be established and used to define more aspects of the role of BMP-9 in colorectal tumours.

6. Materials and Methods

6.1 Patient tissue samples

We obtained all human tissue samples from University Hospital Mannheim. All the patients involved were informed and permission for tissue procurement was achieved from local Medical Ethics Committees. Matched colon biopsies (cancer and non-cancer areas) were taken from each patient in the II Medical Clinic of the University Hospital Mannheim (internal patient ID's: P018, P055, P080 for CAFs-Organoids co-culture experiments and P080, P082, P090 for BMP-9 stimulation experiments), (Reference No. 2014-633N-MA and 2016-607N-MA). Human liver tissue was collected from cancer-distant areas of resection samples from HCC or CRC liver-metastases patients (Reference No. 2012-293N-MA).

6.2 Mutation status analyses

Amplicon sequencing was performed as reported previously[59]. Exome sequencing was performed according to the standard pipeline of the core-facility of the DKFZ, Heidelberg.

6.3 Mouse tissue samples

Five C57BL/6 mice, which are from the control group of BMP-9 knockout mice were sacrificed, liver and colon samples were taken, after RNA isolation, q-PCR was performed for BMP-9, ALK1 and ID1 expression comparisons. They are all wild-type, male mice, by sacrificing at the age of 4-5 months and an average weight of 34 g. Liver and colon tissue from the same mouse were earned and washed with PBS for three times, after cut into small pieces they were immediately frozen in liquid nitrogen for later RNA purification (see below). BMP-9 knockout mice were sacrificed, intestine samples were taken for Immunofluorescence (see below). The mice are a gift from our cooperation partners: Aranzazu Sanchez Munoz and Blanca Maria Herrera

Gonzalez, Department of Biochemistry and Molecular Biology, Faculty of Pharmacy, Complutense University of Madrid Plaza Ramón y Cajal S/N, 28040-Madrid, Spain.

6.4 Generation of Normal Organoids (N-Orgs)

Six to ten fresh human tissue biopsies per each patient (Table 2) were taken from patients who went through colonoscopy in the II. Medical Clinic of the University Hospital Mannheim. Samples were directly preserved in Phosphate-buffered saline (PBS) on ice and transferred to the lab as soon as possible. Then they were gently washed with PBS on ice six times: the first three times in a petri dish and the last three times in 15 ml falcon tubes. Tubes were standing on ice, letting the tissue sink to the bottom, then discarding the supernatant. A sharp pair of scissors was used for cutting the biopsies into 2-4 mm^2 pieces. The pieces were washed in Advanced Chelation Solution (ACS: 5.6 mM Na2HPO4, 8 mM KH2PO4, 96.2 mM NaCl, 1.6 mM KCl, 43.4 mM Sucrose, 54.9 mM D-sorbitol) for another three times similar to the second washes in PBS. An incubation medium made of ACS plus EDTA (40 uL of 2 mM Ethylenediaminetetraacetic acid (EDTA) in 10 mL ACS) was prepared in 15 ml falcons. Tissues were then incubated at 4 °C for 1h on a rotating machine. After gentle pipetting, 10 µl of the sample were taken and the number of crypts in solution was counted. If it was less than 2 crypts/µL, the incubation time was extended. After filtering through a 100 µm filter, crypts were centrifuged at 150 g, 4 °C for 10 min. The supernatant was discarded and 100 µl/well matrigel was pipetted on ice. In the form of drops, 1500 crypts were mixed with 100 µl matrigel and were pipetted into one well of a pre-warmed six-well suspension plate. The six-well plate was placed upside-down in a 37ºC, 5% CO_2 incubator for 45 min. After that, the matrigel had solidified, drops were formed and were tightly sticking to the bottom. 2 ml WENRA medium (Table 3) was added per well. After 24h the first medium change was performed and then every 48-72 h.

6.5 Generation of Tumour Organoids (T-Orgs)

Human CRC biopsies were treated as described above for normal tissue except the following difference: cutting of the tissue should be more careful. Liberase (13 U/mL dissolved in PBS) was used for the initial dissociation at 37°C for one hour or until a

concentration of more than 2 cells/µL was achieved. After filtering through a 100 µm filter, cells were centrifuged by 200 g, 4°C, 5min. 200 000 cells per 100 µl of Matrigel were pipetting in forms of drops in one well of a six well suspension plate. Expansion medium used was ENA.

6.6 Organoids culture

After initial generation, Organoids were first expanded before BMP-9 stimulation or co-culture experiments. Culture medium was freshly prepared before use and stored in 4 °C for no more than two weeks. WENRA medium (Table 3) was used for normal Organoids (N-Orgs) and ENA (Table 3) was used for Tumour Organoids (T-Orgs). To passage Organoids they were scratched off with the matrigel drops from the six well plates using a cell scraper and were collected in a 15 ml falcon tube. After centrifugation at 800g, 4 °C for 3 minutes, the supernatant was discarded and the pellets were collected on ice. 1 ml trypsin EDTA (ThermoFisher scientific) was pipetted to the pellet and mixed thoroughly before incubation at 37°C in a water-bath for 10 minutes. Incubation was stopped by adding FCS and the Organoidsuspension was centrifuged at 800g, 4 °C for 3 minutes. The pellest were resuspended in 100 µl/well matrigel and were transferred into pre-warmed six-well plates as described above. The six well plate was placed again upside-down in a 37ºC, 5% CO_2 incubator for 45 min and then 2 ml WENRA/ENA medium (Table 3) was added per well. Medium was changed every 48-72 h.

6.7 Freezing and thawing of Organoids

When Organoids fully populated the matrigel drops, but did not yet grow out from the matrigel, they were ready for freezing. All the matrigel drops were scraped from the bottom of the six well plate and collected in a 15ml falcon. Under the centrifuge condition of 800g, 4 °C for 3 minutes, pellets were collected and were resuspended in 1 ml/cryo-tube in medium which consisted of 90% FCS and 10% DMSO. All the resuspension work was done on ice and cryo-tubes were then transferred to “Mr. Frosty” containers for 24h in -80° freeezers and afterwards they were stored in -80 °C freezers or Liquid Nitrogen Tanks.

To thaw organoids, the cryo-tubes were put for not more than 2 minutes in a pre-warmed 37 °C water bath so that the freezing medium would melt. Organoids were then collected in 10 ml pre warmed Advanced DMEM/F12 containing 10% FCS. Samples were centrifuged again at 800g, 4 °C for 3 minutes and pellets were resuspended in 100 µl/well matrigel in 6-well suspension plates. After thawing, organoids were passaged at least one time before experiments were performed.

6.8 Isolation of CAFs

Human CRC biopsies were processed as described above for normal tissue until cutting of the tissue into 2-4 mm^2 pieces. After washing with PBS for another three times, the pieces were placed into six-well tissue culture plates and were overlaid with 1 ml DMEM (containing 10% FCS) per well. Plates were kept at 37ºC, 5% CO_2 for 24 h followed by a medium change using now 2 ml of DMEM (+10% FCS) per well. After 24-48 h fibroblasts grew out at the edges of the tissue and were further amplified by monolayer culture. The medium was exchanged every 48-72 h.

6.9 CAFs culture

CAFs were cultured in DMEM medium (containing 10% FCS, 1% penicillin, streptomycin and 1% Glutamine) in tissue-culture treated 75 cm^2 culture flasks and the medium was changed every 48-72h. When passaging cells were first washed three times with warm PBS and then 1 ml trypsin was added on top of the attached cells. Digestion was processed in 37ºC, 5% CO_2 incubator and the cells are being closely observed under the microscope until they dis-attached. 10% FCS DMEM medium was then added and the cells were collected in falcons. After centrifuge in 1500 rpm, 25°C for 5 minutes, the pellet was resuspended in the above described culture medium and plated into cell culture flasks again.

6.10 Freezing and thawing of CAFs

When CAFs were 85-90% confluent in a 75 cm^2 flask, they were ready for freezing. The old culture medium was discarded and pre-warmed PBS was used for three times of washing. Dislodging of the cells was performed by adding 1 ml Tripsin LE at 37ºC, 5% CO_2. After centrifugation (1500 rpm, 25°C for 5), the pellet was resuspended in 70% DMEM +20% FCS +10% DMSO medium and approximately 1 Mio. cells in 1ml freezing medium was pipetted on ice into cryo-tubes. After 24h in "Mr. Frosty" containers in -80°C, they were moved into a -80 °C freezer or Liquid nitrogen tank. For thawing, cryo-tubes were shortly shaken in a pre-warmed 37 °C water bath for 2 Minutes. CAFs were collected then in 10 ml pre warmed DMEM plus 10% FCS medium. After centrifuge at 1500 rpm, 25°C for 5 minutes pellets were resuspended into DMEM medium (10%FCS+1% penicillin, streptomycin+ 1%Glutamine) and plated in flasks again.

6.11 Isolation of RNA from cells, tissue or Organoids

Attached cells were washed with pre-warmed PBS for three times and then lysis buffer was pipetted directly on top of the cells (Peqlab). A cell scraper was used to collect as much sample as possible. Already cut frozen tissue samples were transferred to lysis buffer and were disrupted by mechanical homogenization on ice. Organoids in Matrigel droplets were scratched off from the dish and collected in falcon tubes. After centrifugation at 4ºC, 800 g for 3 min, Lysis buffer was added directly to the pellet containing the Organoids followed by gentle vortexing for 1 min. PeqGOLD Total RNA purification kit (Peqlab) was used for RNA extraction as indicated by the manufacturer's instructions.

6.12 Real-time PCR

RNA concentration and purification were measured after extraction. Then the SensiFAST cDNA Synthesis Kit (Bioline, UK) was used for reverse transcription of the RNA into single-stranded cDNA. Real time PCR (qPCR) was carried out according to Analytik Jena innuMIX qPCR Master mix SyGreen protocol (Jena, Germany). RT-PCR primers were either generated by a software or purchased (Qiagen, Germany). The

sequences used are listed in Table 4. Different housekeeping genes (HKG) were used for normalization and are also listed in Table 4.

6.13 Immunofluorescence

Organoids or tissue were buried in paraffin blocks and cut into 3 µm per slide. After dewaxing and rehydration, Antigen retrieval was performed using unmasking solution (Cole Parmer). After small bubbles can be seen, the slides were heated at 180W for 10 minutes in a microwave and were then cooled down at room temperature. After washing with PBS an addition of 100% FCS for blocking of unspecific binding sites was followed. The primary antibody against Ki67 (proteintech) was diluted 1:1000 in PBS and the slides were incubated with the 1st antibody at 4ºC overnight. In the Second day, slides were first washed with PBS and then incubated with the secondary antibody which was diluted 1:350 in 10% FCS/PBS for 1h at room temperature. Then Draq5 diluted in 1:1000 (Biolegend) was pipetted on top of the samples and incubated in the dark for 10 minutes. In the end DAKO mounting medium was used to cover the sections and the slides were stored in the dark at 4ºC. Confocal microscopy was used for imaging and Image J was used for quantification of the positive staining signal.

6.14 Western blot

T-Orgs were dissolved in lysis buffer [one Protease inhibitor cocktail tablet (Roche, Germany) was dissolved in 10 ml PPRI (1x Tris-buffer saline, 1% Nonidet P40, 0.5% sodium deoxycholate, and 0.1% sodium dodecylsulfate in water, mixed with 100 µl phosphatase inhibitor cocktail2 (Sigma)) and centrifuged at 12.000 rpm, 4ºC for 10 min. Supernatants were colorimetrically quantified using a BioRad protein quantification assay (BioRad, Munich, Germany) and stored at -20 ºC. Pre-cast polyacrylamide gels (Thermo Fisher) were loaded with equal amounts of protein (30 µg/lane), and after electrophoresis they were transferred to nitrocellulose membranes (Pierce Rockford, IL, USA). Transfer was visualized by Ponceau Red staining. Primary and secondary antibodies (P-Smad1: Abcam; Beta-actin and secondary antibodies: Santa Cruz Biotechnology) were diluted as recommended by the manufacturer.

Chemiluminescence was detected using a Fusion solo chemiluminescence detection system (Vilber lourmat).

6.15 Micro-array analyses

After RNA extraction, RNA concentration and quality were checked. Samples whose RIN values were above 7.8 were prepared into 100 ng/µl and a total volume of 10 µl was used. cDNA was hybridized to Clariom S Human Microarrays (Affymetrix, Santa Clara, CA) at the Institute of Medical Research Center (Medical Faculty Mannheim). Raw intensity CEL files measured with the Affymetrix instrument were read by the oligo package in R/Bioconductor. Background substraction, quantile normalization and summarization were performed by Robust Multichip Average (RMA) algorithm. Application of quantile normalization was performed for the adjustment of distributions of expression levels between arrays. Differentially expressed genes (DEGs) were determined using the R package limma. The GESA software were used for Gene Set Enrichment Analysis (GSEA) based on the differential expression profiles and canonical pathways gene sets derived from the KEGG (Kyoto Encyclopedia of Genes and Genomes) pathway database that were collected by the molecular signatures database (MsigDB). A self- defined gene set used for detecting a BMP-9 pathway enrichment contained the following genes: *ACVRL1, ACVR1, BMPR1A, BMPR1B, ACVR2A, ACVR2B, BMPR2, ENG, SMAD4, SMAD1, SMAD5, SMAD9, ID1, ID3*. Only when the false discovery rate (FDR) was lower than 0.25 and the P-value was lower than 0.05 the results were considered to be statistically significant. CMS subtypes were determined using the CMSCaller R package[60].

6.16 Live/dead staining of Organoids in culture

Colorectal non-tumour Organoids were recovered from -80°C and plated in WENRA. After one passage, cells were plated in 12 well-plates, again in WENRA. 24 h later the medium was changed to either WENRA again, Advanced medium or Advanced medium +10% DMSO (positive control for cell death). 48 h later, 0.1 µM Calcein-AM (Biolegend) was added directly to the wells followed by incubation in the dark at 37°, 5% CO_2 for 30 minutes. Then 10 µg/ml Propidium iodide (Biolegend) was added

followed by another incubation in the dark at 4°C for 15 minutes. An AXIOVert A1 microscope from ZEISS was used for imaging (Time-points: subsequently to staining (= 48h) and one day later (= 72h)). For quantification, dead cells within individual Organoids were counted in 20 fields.

6.17 Analysis of gene expression databases

Gene expression patterns between normal and tumour tissues were analysed by GENT (http://gent2.appex.kr/gent2/). The effects of the ID1 and Noggin expression levels on the Patients Disease Free Survival times were determined using GEPIA (http://gepia.cancer-pku.cn). The TCGA-COAD+READ cohorts were analyzed and the high/low cutoff value was 50%. Protein-Protein interaction networks were analyzed using STRING (https://string-db.org/).

6.18 Statistics

Figures and statistics were generated using GraphPad Prism 8.0a (GraphPad Software Inc., San Diego, CA, USA). Experiments were performed at least in triplicates (3 independent experiments) and un-paired two-sided t-test was used for determination of significance of differences between groups. Error bars are standard deviation and $p<0.05$ was considered statistically significant (*).

7. Results

Large parts of these data were included in our resulting publication:

Cai C, Itzel T, Gaitantzi H, de la Torre C, Birgin E, Betge J, Gretz N, Teufel A, Rahbari NN, Ebert MP, Breitkopf-Heinlein K. *Identification of liver-derived bone morphogenetic protein (BMP)-9 as a potential new candidate for treatment of colorectal cancer.* J Cell Mol Med. 2022;26(2):343-353. PMID: 34841646.

7.1 The BMP-pathway plays a role in CRC

7.1.1 BMP-9 is expressed in lower levels in Colorectal cancer patients as compared to the healthy control group.

To know better the function of the BMP-pathway in cancer, especially in CRC, we started with an in silico analysis of BMP-9 expression patterns in patient tissue samples using the GENT database. We found that BMP-9 is significantly higher expressed in normal tissue as compared to cancer tissue in Adrenal-Gland, Bladder, Breast, Cervix, Kidney, Larynx, Liver, Pancreas, Stomach, Tongue, Urothelium and Colon tissue. In Blood and Uterus tissue however, the opposite relation was found (Fig. 2).

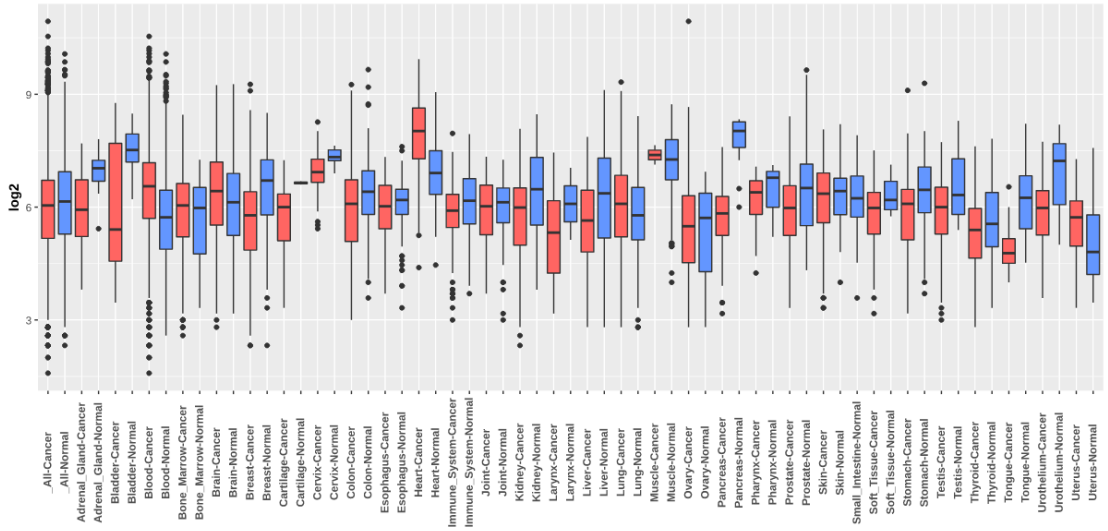

Fig. 2: In silico analysis of BMP-9 expression in cancer tissue versus normal tissue. The BMP-9 expression profile was analyzed in different cancer samples using the GENT GPL96

platform (HG-U133A). In colon cancer patients lower expression of BMP-9 was found in the tumour as compared to the corresponding non-tumour control ($p<0.001$).

7.1.2 In silico analyses show that high expression of the BMP-target gene ID1 and low expression of the BMP-inhibitor Noggin leads to better overall survival of CRC patients

We searched for in silico data to better understand the relationship between the BMP pathway activity and the patients' disease-free survival times. Noggin is an inhibitor of many BMPs, including BMP 2, 4, 5, 6 ,7[61]. Therefore, Noggin expression was used as an indicator for potentially inhibited BMP signaling whereas expression of the BMP-target gene Inhibitor of Differentiation (ID)-1 was used as an indicator of an active BMP-pathway. 181 patient samples from the Cancer Genome Atlas (TCGA; cohorts colon adenocarcinoma (COAD) plus rectum adenocarcinoma (READ)) were analyzed by GEPIA. As shown in Fig. 3, higher expression levels of ID1 correlated with better patient disease free survival times than lower levels. The relationship between Noggin and patient survival was analyzed in a similar way. 173 samples with high Noggin expression were included and 158 with low Noggin expression. Opposite to ID1, higher Noggin expression correlates with decreased patient disease free survival times. These data gave us a first hint that activation of the BMP pathway could be beneficial for CRC patients.

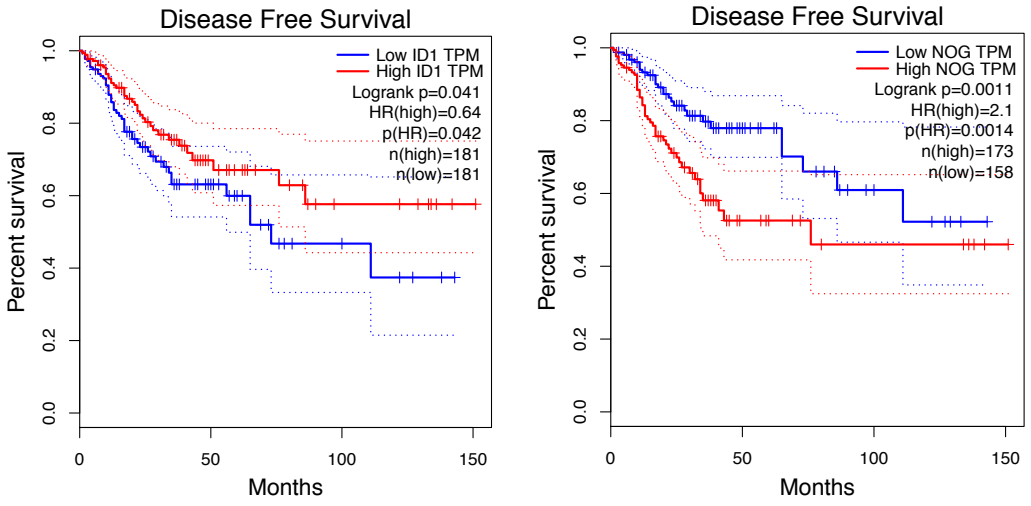

Fig. 3: In silico analysis of ID1 or Noggin expression levels in correlation with patients' disease-free survival times in colorectal cancer (CRC). Results are presented as Kaplan-Meyer curves and demonstrate the prognostic value of the mRNA levels of ID1 (left graph) and Noggin (right graph) in CRC patients' samples. High levels of ID1 expression show a significant correlation (p=0.041) with longer disease-free survival times whereas high Noggin expression shows the opposite effect (p=0.0011). Data were analyzed by GEPIA and TCGA-COAD+READ cohorts (colon plus rectum adenocarcinoma) were used.

7.1.3 BMP-9 is highly expressed in liver while its receptor ALK1 and its target gene ID1 are highly expressed in colon

RT-PCR was used to comparatively analyze the basal expression levels of BMP-9, its receptor ALK1, and its target gene ID1 in non-malignant liver and colon tissue samples from humans as well as mice (Fig. 4). We found that, BMP-9 is higher expressed in liver than in colon. However, ALK1 and ID1 are higher in colon tissue, leading us to the hypothesis that, BMP-9 produced by the liver, may circulate through the bloodstream and regulate target gene expression in the colon. And this cross-talk could be relevant for CRC development or progression.

A B

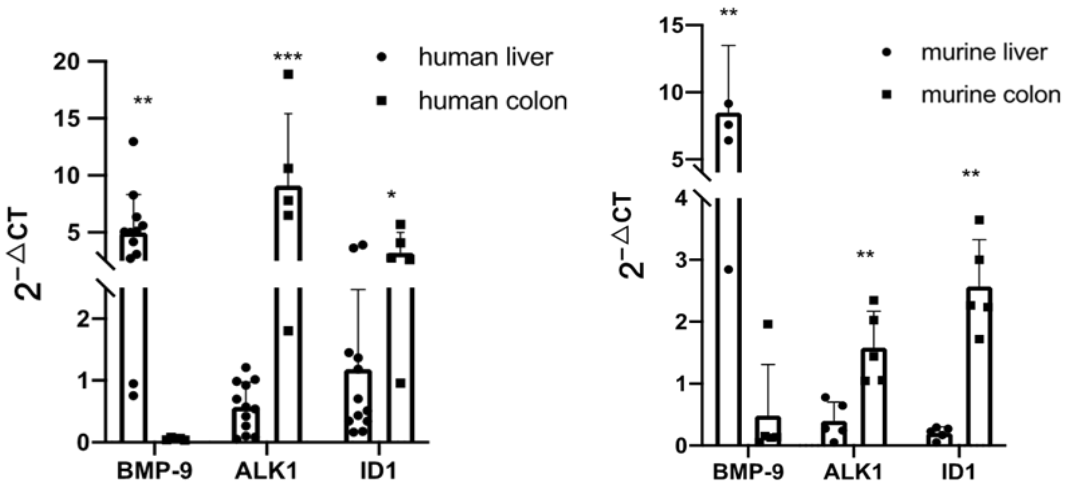

Fig. 4: BMP-9 is mainly expressed in liver, while ALK1 and ID1 are highly expressed in colon. A) 12 human liver samples and 6 human colon samples (both from non-malignant areas)

were collected and processed for RT-PCR. CT values for BMP-9, ALK1 and ID1 were normalized to the house-keeping gene rS18. B) 4 mouse liver samples and 5 mouse colon samples were obtained from healthy mice and processed for RT-PCR analyses. CT values for BMP-9, ALK1 and ID1 were normalized to the house-keeping gene b2M. Statistically significant changes are indicated as follows: p>0.05: (*); p>0.01: (**); (p>0.001): (***).

7.2 Generation of epithelial Organoids from normal and cancerous biopsies of individual colorectal cancer patients

7.2.1 Generation of gut epithelial Organoids

In order to obtain a human, 3-dimensional in vitro model system for colon, we generated Organoids from patient biopsies donated by three colorectal cancer patients, basically according to previously published protocols[46]. In contrast to most previous publications we focused on the direct comparison of Organoids derived from normal as well as cancerous samples from the same patient. We used a slightly modified recipe for stem-cell supporting media (using ENA and WENRA, see materials and methods for composition) only initially when the Organoids first develop and are being amplified. Since these media contain many different cytokines and inhibitors that might finally interfere with the effects that we want to analyse (in this case the response to BMP-9), we changed the culture medium to an "Advanced" medium (containing strongly reduced amounts of cytokines and growth factors) two days before analyses (Figure 5).

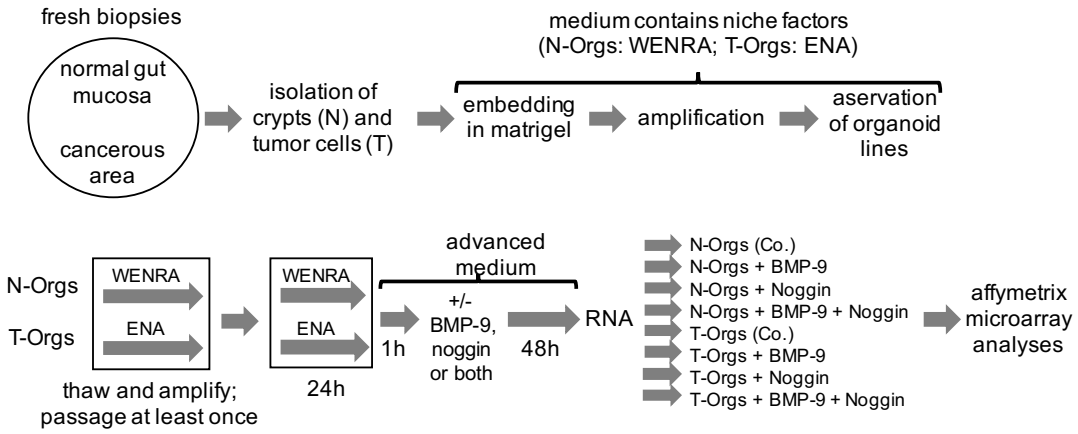

Fig. 5: Schematic presentation of the experimental work-flow. A) Generation of Organoids from normal (N) and cancerous (T) areas using colon biopsies from the same patient. For generation of optimal growth conditions, the Organoids were cultured in medium containing defined factors of the stem cell niche of the colon crypts (WENRA for N-Orgs and ENA for T-Orgs; see materials and methods section for exact composition). B) After thawing the organoid lines, they were first amplified and after at least one passaging they were cultured for 24h in their corresponding amplification media and one hour before stimulation with BMP-9 (5 ng/ml) or Noggin (100 ng/ml) or both, the medium was changed to an advanced medium (see materials and methods for details). After two further days total RNA was isolated and processed for Affymetrix microarray analyses.

7.2.2 Organoids morphology is not changed after culture for 72 hours in Advanced medium.

Before starting with stimulation experiments, we first wanted to prove that Advanced medium is suitable for the culture of Organoids for a short time. We started with observing the morphology of Organoids. As shown in Fig. 6, both N- and T-Orgs can be cultured in Advanced medium for at least 72 hours without any obvious morphological changes. However, probably due to the lack of pro-proliferative cytokines, they grew slower in Advanced medium as compared to ENA or WENRA (data not shown).

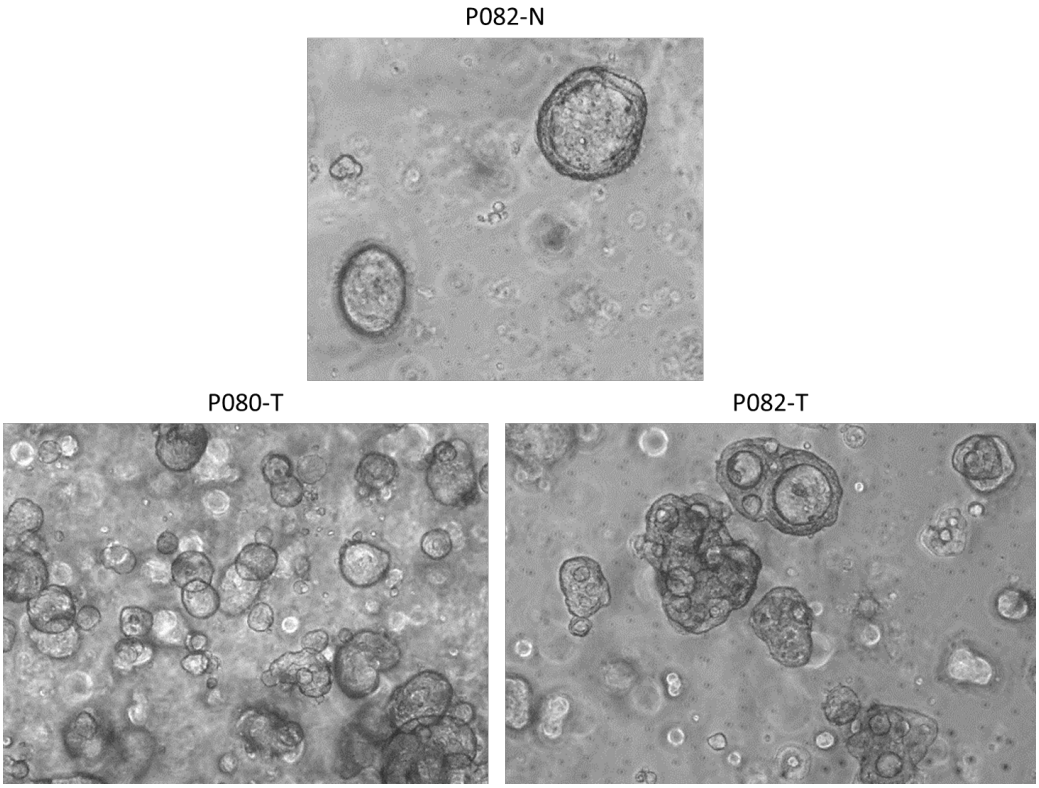

Fig. 6: Morphology of N- as well as T-Orgs in Advanced medium. 3 days after changing the medium to Advanced medium, the morphology of N- as well as T-Orgs was observed under phase-contrast microscopy. Magnification 40X.

7.2.3 Organoids viability is not reduced by culturing Organoids in Advanced medium

To further support the morphologic observations that culturing Organoids in Advanced medium does not negatively affect the cells' viability, we analyzed the amount of cell death using a quantitative measure, a so called "live/death staining assay". N-Orgs were cultured in Advanced medium or in WENRA for 72 hours and Advanced medium plus DMSO was used as positive control for induced cell death. Photos of the resulting fluorescent stainings show clear apoptosis (red colour, stained by Propidium iodide) in Advanced plus DMSO medium but not in the other two groups (Fig. 7A). This change in viability was already visible by bright-field microscopy (Fig 7B). Quantification of dead and living cells again showed no statistically significant difference between WENRA and Advanced medium after 48 or 72 h (Fig 7C), supporting the conclusion

that culturing these Organoids in Advanced medium for up to 72 h does not compromise their vitality.

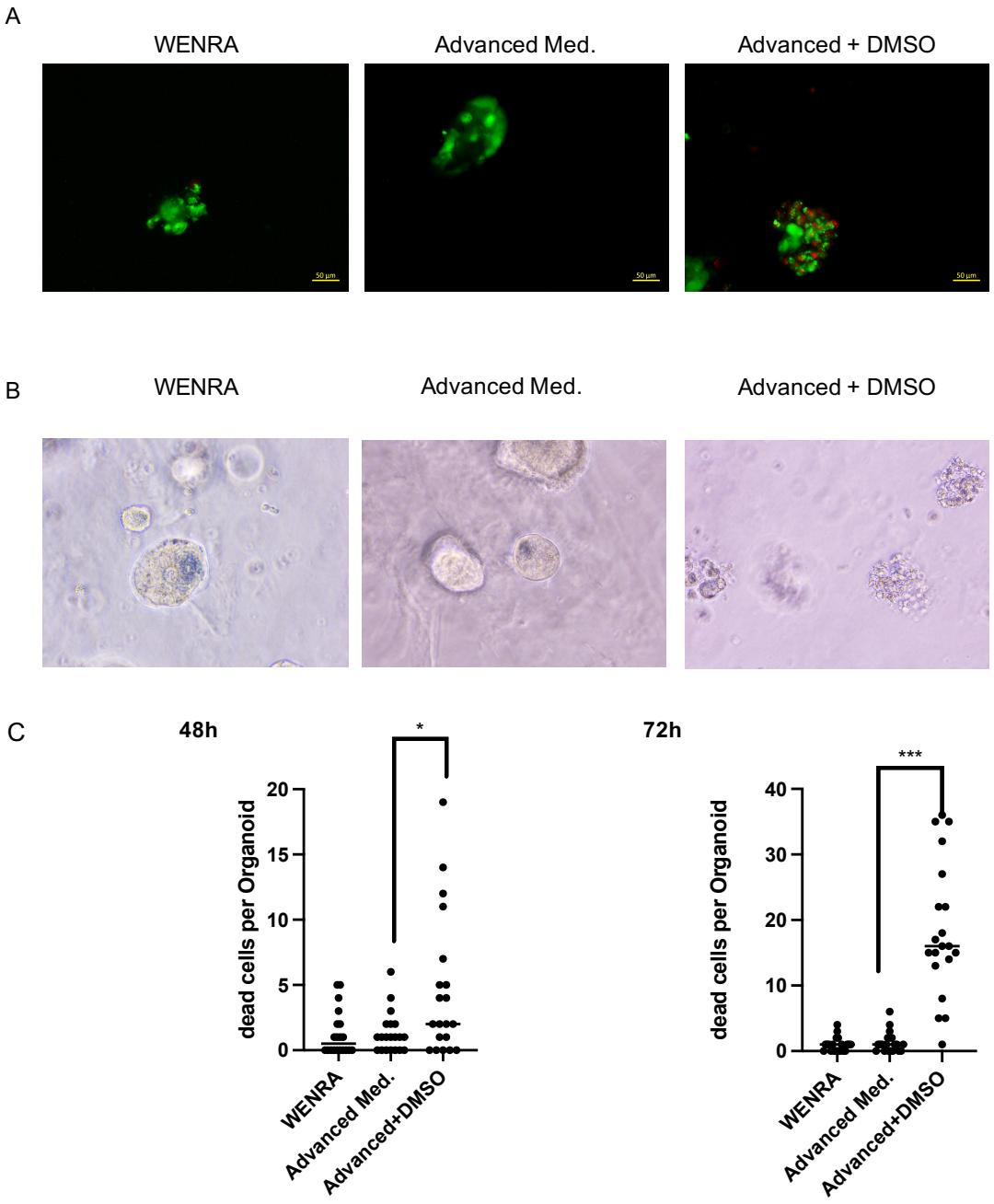

Fig. 7: Live/dead staining of colorectal Organoids (non-tumour) cultured in Advanced medium. N-Orgs were recovered from -80°C and were plated as described in Fig. 5. One condition with Advanced medium plus 10% DMSO was included as positive control for cell death induction. Calcein-AM (0.1 µM) and Propidium iodide (10 µg/ml) were added directly into the culture medium as described in methods. The Organoids' viability was documented

microscopically (green = alive; red = dead). A) Representative pictures of stained Organoids after 48h. The scale bar represents 50 µm. B) Representative bright-field pictures (72h). C) Quantification of dead cells per individual organoid (20 fields per condition were analyzed at 48 and 72h). *$p<0.05$ and ***$p<0.001$ as determined by t-test

7.2.4 Functionality and differentiation-markers are upregulated in Organoids cultured in Advanced medium as compared to ENA

RT-PCRs against general viability markers as well as markers of epithelial functionality were performed after 3 patients' tumour Organoids were either cultured in ENA or in Advanced medium for 72 h. As expected, PCNA, a marker for proliferation was reduced in Advanced medium. Bcl2 was also down-regulated in 2 of the 3 patients and the pro-apoptotic protein BAX was slightly enhanced. Nevertheless, general functionality- and differentiation-markers like CA1, SLCA5 and FABP were all upregulated, supporting our assumption that the Organoids indeed survived and remained differentiated and functional also in Advanced medium (Suppl. Fig. 3).

7.2.5 Colon Organoids are responsive to BMP-9 stimulation

Using Organoids, we then investigated whether the BMP/Smad-1 pathway can be activated by BMP-9 in normal as well as malignant gut epithelium. As shown by Western blot, after stimulation with BMP-9 the BMP signal transducer Smad1 is activated by phosphorylation in the T-Orgs of patient 80 (Fig. 8A). Furthermore, we performed micro-array analyses from samples of N- and T-Orgs and found that in BMP-9 stimulated Organoids there is a significant enrichment of TGF-β pathway related gene expression with an enrichment score of 1.85 and 1.47 in N- and T-Orgs, respectively (Fig. 8B). We next defined a group of BMP-9 regulated genes (see materials and methods) and performed again gene set enrichment analyses. Under a strong statistic control of FDR being lower than 0.25 and a P value lower than 0.05, we still found that human colon Organoids are clearly responsive to BMP-9 (Fig. 8C).

A

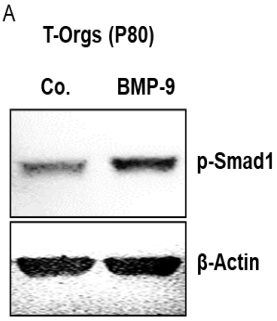

B

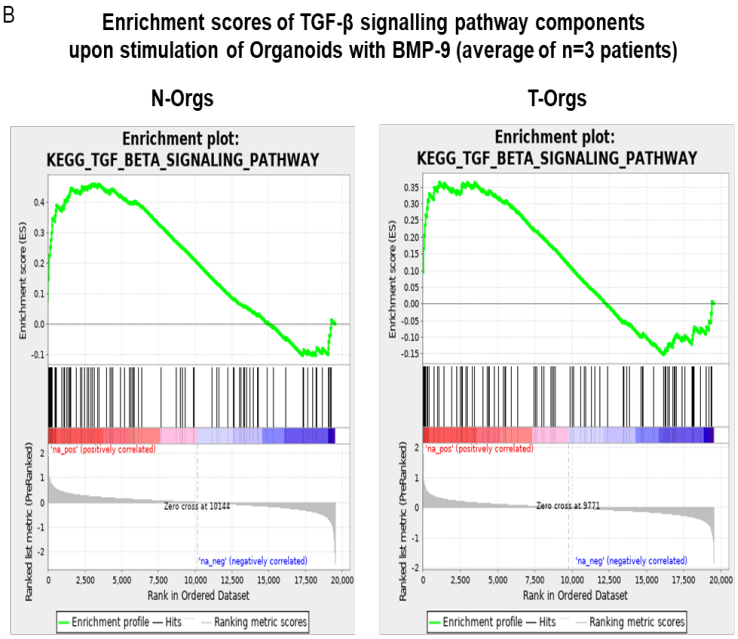

C

Enrichment scores of BMP-9 signalling pathway components
upon stimulation of Organoids with BMP-9 (for each patient individually)

NAME	SIZE	BMP-9_Normal_P80			BMP-9_Normal_P82			BMP-9_Normal_P90		
		SIGN	NOM.p.val	FDR.q.val	SIGN	NOM.p.val	FDR.q.val	SIGN	NOM.p.val	FDR.q.val
BMP-9 SIGNALLING	13	1	0.0000	0.0033	1	0.0068	0.0207	1	0.0206	0.0913
NAME	SIZE	BMP-9_Tumour_P80			BMP-9_Tumour_P82			BMP-9_Tumour_P90		
		SIGN	NOM.p.val	FDR.q.val	SIGN	NOM.p.val	FDR.q.val	SIGN	NOM.p.val	FDR.q.val
BMP-9 SIGNALLING	13	1	0.8034	1.0000	1	0.0260	0.0560	1	0.0000	0.0000

Fig. 8: BMP9-response of N- and T-Orgs. A) Western Blot using lysates from T-Orgs (P080) +/- BMP-9 stimulation. Phosphorylation of Smad1 demonstrates that BMP-9 signalling was successfully initiated. Beta-actin was used as loading control. (B) After stimulation with BMP-9, a Normalized Enrichment Score (NES) for the TGF-β signature of 1.85 and 1.47 was observed in N- and T-Orgs, respectively. (C) A group of BMP-9 regulated genes was defined (see materials and methods) and the single patients' enrichment scores for this signature were calculated. 1 stands for enrichment in BMP-9 stimulated versus unstimulated Organoids. Green means statistical significance: a false discovery rate (FDR) lower than 0.25 or a P-value lower than 0.05 (yellow).

7.3 Characterization of epithelial colorectal normal as well as tumour Organoids

7.3.1 Cell type marker expression in N-Orgs and T-Orgs

For the generation of Organoids we initially isolated crypts or stem-like progenitor cells from colon biopsies. These cells are responsible for renewal of the lining of the colon. Therefore, one could expect that non-epithelial cells should be absent. To check the purity of our Organoids, we proceeded with analysing the micro-array data and investigated the expression levels of different cell type markers. Expression levels of a selection of classical differentiation markers is shown in suppl. Fig. 4A. As shown in Suppl. Fig 4B, the N-Orgs mainly expressed epithelial and stem cell markers. Fibroblasts and endothelial cell markers were barely expressed, indicating the epithelial purity of our Organoids. Also in T-Orgs a similar expression pattern was observed (Suppl. Fig. 4B).

7.3.2 Consensus molecular subtypes of T-Orgs

Consensus molecular subtyping is an RNA expression-based classification system for colorectal cancer (CRC) that can be used as a tool to improve clinical precision. Four types of CMS are normally used: CMS1 is associated with microsatellite instability and immune infiltration. CMS2 and CMS4 are characterized by chromosomal instability, in which CMS2 shows activation of the Wnt and Myc pathways and CMS4 is described as a mesenchymal stroma-rich group having poor prognosis. CMS3 patients have dysregulated metabolism[62].

To identify the subgroups of the tumours of the 3 patients used here, "CMScaller", an R package was used as described by Eide et al.[60]. Our results show that P080 belongs to CMS1 with high statistical significance and P082 belongs to CMS3 with an intermediate P-value (Suppl. Fig. 5A). P090 which has a TP53 mutation (Suppl. Fig. 6) was suspected to be either CMS2 or CMS4, this fits to the previous findings stating that the TP53 mutation frequency is highest in CMS 2 and 4[63]. And we also proved it again by in silico data: our data show that in TP53-mutated group 48.82% are CMS 2 and 31.18% are CMS 4 (Suppl. Fig. 7). In non-TP 53 mutated group however, the percentage of CMS 2 and 4 are 22.7% and 28.37% seperatrly (data not shown here).

As mentioned above, CMS2 shows activation of the Wnt pathway. But in P090 the Wnt pathway was deactivated because of the APC gene mutation (APC expression levels

were also much lower as compared to the other patients (Suppl. Fig. 6)). Smeby et al. also showed that TP53 mutation in CMS4 leads to enhanced proliferation. P090 showed enhanced expression of the proliferation marker genes PCNA and MKI67, and reduced expression of the anti-proliferative CDKN1A (Suppl. Fig. 5B), suggesting that P090 possibly belongs to CMS4. Consistent with the fact that CMS4 patients have generally a worse prognosis, our P090 developed metachronous hepatic and pulmonal metastases (Table 2) which is a sign for a rather bad prognosis.

7.3.3 Gene sets enriched in T-Orgs as compared to N-Orgs

Our gene set enrichment analyses showed that gene sets related to cell growth and information processing like replication and repair, transcription, folding, sorting and degradation were enriched in T-Orgs as compared to N-Orgs. Metabolic gene sets including lipid- or amino acid metabolism were also enriched in T-Orgs, whereas those comprising glycan biosynthesis and immune regulation were decreased in T-Orgs (Suppl. Fig. 8). This fit to the common tumor signatures based on gene set enrichment analysis from other scientists[64].

7.3.4 Expression changes within the individual patients

We did fold change analyses for all the three patients and picked out the top 30 up- or down-regulated genes in N- vs. T-Orgs. Patient-specific expression patterns were clearly found in our samples. Of the top 30 down-regulated genes, none were identical between the three tumour Organoid lines. Also, among the up-regulated genes, only few were commonly found in all three patients. One of them was Protein tyrosine phosphatase, receptor type O (PTPRO), a protein that belongs to the R3 subtype family of receptor-type protein tyrosine phosphatases (Suppl. Fig. 9). It might function as a tumour suppressor and decreased expression was observed in several types of cancer[65]. According to our results, however, it is up-regulated in T-Orgs, a finding that deserves further investigations in the future.

7.4 Opposite effects of BMP-9 and Noggin on N- and T- Organoids

7.4.1 Basal expression of the BMP-pathway in T- versus N-Orgs of the individual patients

After the establishment of our experiment model and characterization of the Organoids, we continued to investigate the role of BMP-9 in CRC by stimulating the Organoids with BMP-9, Noggin, or a combination of both (see scheme in Fig. 5). RNA was again isolated and processed for microarray analyses.

The resulting expression profiles showed that the BMP-9 pathway target genes ID1-4 were up-regulated in T-Orgs from patients 080 and 082. However, a strong down-regulation of expression was found in the T-Orgs of patient 090. The BMP-9 co-receptor, endoglin (ENG), was oppositely regulated in the same three tumour patients. The BMP-9 receptors ALK1, ALK2, BMPR1A, BMPR1B, ACTR2A, ACTR2B, BMPR2, the BMP-9 pathway intermediate proteins SMAD1, SMAD5 and the BMP inhibitor Noggin were mainly unchanged (Fig. 9A). Expression changes of ID1, ID3, and endoglin (ENG) were further verified by regular real-time PCR (Fig. 9B).

A

	T-Org vs. N-Org(FC)		
	P80	P82	P90
ACVRL1	-0.10	-0.63	-0.45
ACVR1	-0.26	0.10	-0.64
BMPR1A	-0.52	0.38	-0.04
BMPR1B	-0.08	0.03	0.00
ACVR2A	-0.54	0.42	-0.50
ACVR2B	-1.51	0.80	0.02
BMPR2	-0.43	-0.12	-1.05
ENG	-0.19	-0.22	1.33
SMAD1	-0.48	-0.50	-0.69
SMAD5	0.23	0.27	-0.88
SMAD9	0.20	2.05	-1.86
ID1	2.18	3.51	-5.88
ID2	1.52	1.28	-2.68
ID3	3.37	2.96	-3.92
ID4	1.07	0.52	-1.85
NOG	0.15	-0.17	-0.19

B

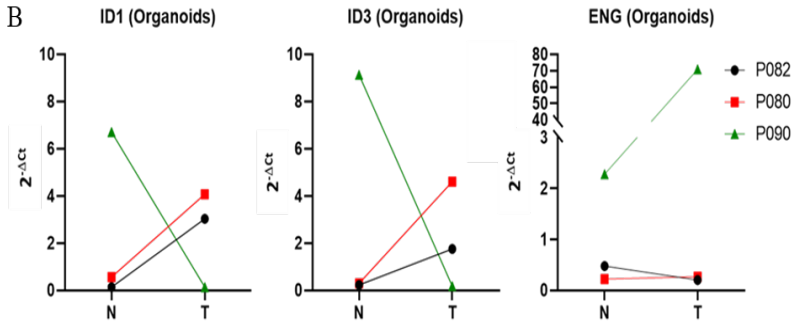

Fig. 9: Analyses on the expression changes of the BMP-pathway in T-Orgs derived from 3 colorectal cancer patients. A) Expression changes of BMP-pathway receptors, co-receptor endoglin (ENG) and target genes ID-1 to -4, the BMP-inhibitor Noggin (NOG) in T-Orgs compared to their corresponding N-Orgs are shown. Up-regulated expression is shown in green, down-regulated in red ($P<0.05$ was considered as statistic significant). Individual fold changes (LogFC) of each patient as calculated from array analyses are given. B) Verification of the array data by regular real-time PCR: Expression changes for ID1, ID3 and ENG closely matched the corresponding array data.

As mentioned above, higher ID1 expression is associated with better patient outcome. Our patient 090, in which the basal expression of ID1 in the T-Orgs as compared to N-Orgs was strongly down regulated, showed more aggressive tumour behaviour, in terms of liver- and lung- metastases formation (Table 2).

7.4.2 BMP-9 signaling antagonizes the expression of genes related to cell growth in N- and T- Organoids

Organoids were stimulated with BMP-9 and/or Noggin and gene set enrichment analyses were performed using the resulting array data. As shown in Fig. 10, gene sets related to immune response as well as lipid- and carbohydrate-metabolism were enriched in BMP-9 treated N-Orgs, while genes responsible for cell growth and cell cycle progression were higher enriched in the unstimulated N-Orgs. Interestingly, similar results were found in T-Orgs, indicating a tumour-suppressive effect of BMP-9 in both N- and T-Orgs (Fig 10A).

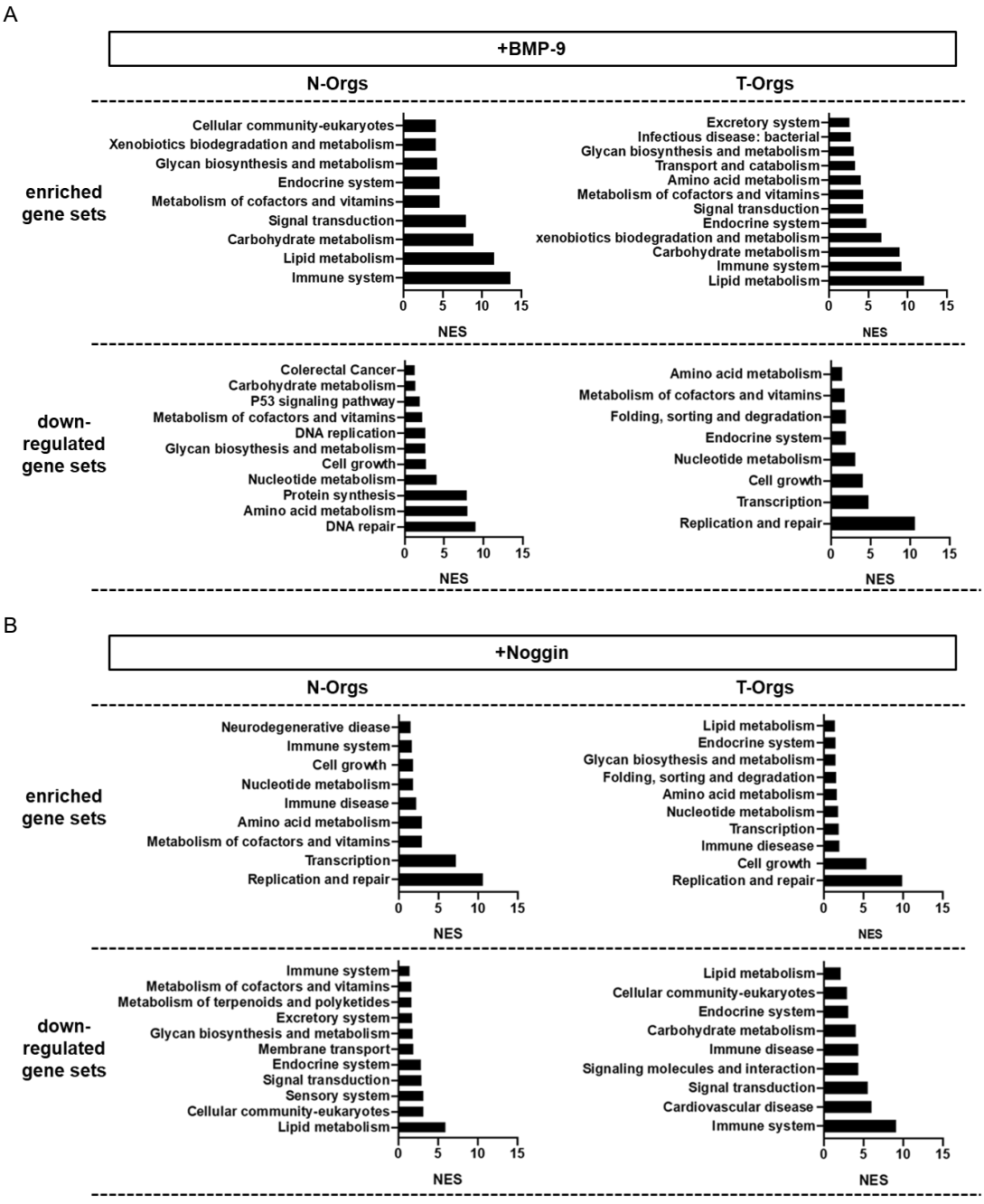

Fig. 10: BMP-9- and Noggin-responses of N- and T-organoids. After stimulation of organoids with (A) BMP-9 (5 ng/ml) or (B) Noggin (100 ng/ml) for 48h, Gene sets enrichment analyses (GSEA) were performed focusing on the Kyoto Encyclopedia of Genes and Genomes (KEGG). A false discovery rate (FDR) lower than 0.25 and a p-value lower than 0.05 were considered as statistically significant. NES: normalized enrichment score.

7.4.3 Noggin enhances the expression of genes related to cell growth in N- and T-Organoids

When we take a look at gene set enrichment analyses derived from Noggin stimulated Organoids, opposite effects as for BMP-9 stimulation were found. After Noggin treatment, gene sets related to cell growth and cell cycle, as well as those related to immune response and lipid-/carbohydrate-metabolism were negatively enriched in Noggin-stimulated N-Orgs. And again, there were no big differences between N- and T-Orgs. In line with the in silico data shown in Fig. 3, a clear tumour-promoting change was shown by gene sets enrichment assay in Noggin-treated Organoids (Fig 10B).

7.5 BMP-9 restricts tumour growth by inhibiting stem cell proliferation

7.5.1 Ki67 expression is reduced by BMP-9 in T-Orgs

Following the array data which suggested a BMP-9-dependent inhibition of proliferation in both N- and T-Orgs, we performed immunofluorescent (IF) staining of T-Orgs from patient 080 after treatment with BMP-9 alone or in combination with Noggin. Ki67 was used as proliferation marker and Draq5 was used for nuclear counter-staining. Representative pictures, taken by confocal microscopy, showed a clear reduction of Ki67 (green) in the BMP-9-treated group and an enhanced signal in Noggin+BMP-9 stimulated Organoids (Fig. 11A). Quantification was performed by Image J and further supported the conclusion that BMP-9 has an anti-proliferative effect (Fig. 11B).

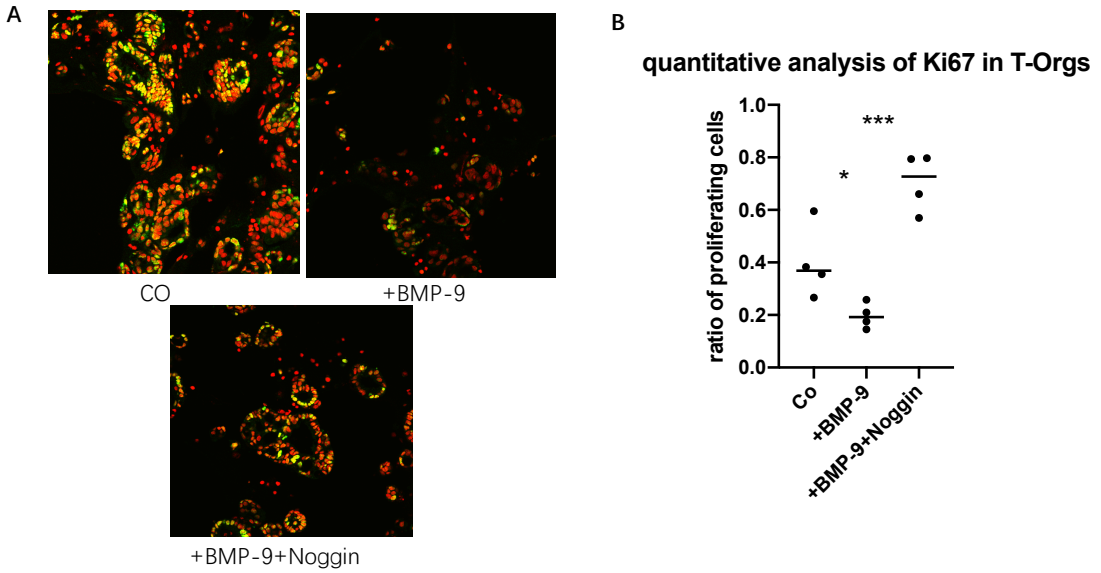

Fig. 11: IF staining of Ki67 in T-Orgs. A) T-Orgs were stimulated by BMP-9 (5 ng/ml) +/- Noggin (100 ng/ml) for 24 hours and IF staining was performed against Ki67(green color) and nuclei were counter-stained with Draq5 (red color). B) Four fields per condition were imaged using confocal microscopy and Image J was used for quantification. *$p<0.05$ and ****$p<0.001$ as determined by t-test.

7.5.2 Enhanced proliferation of stem cells in BMP-9 knockout mice

IF stainings were also performed in tissue samples from BMP-9 knock-out and wild-type mice intestine. More proliferating cells (green) were found in the stem cell area and transit amplifying zone (TA) of the tissue from KO mice as compared to wild-type (Fig. 12A). This fits well with our gene sets enrichment results shown above that indicated that BMP-9 inhibits cell proliferation. The location of these green cells was mainly in the crypt-areas, indicating a possible role of BMP-9 specifically as inhibitor of proliferation of stem cells. By quantification of these stainings using Image J, a statistically significant difference could be demonstrated (Fig. 12B).

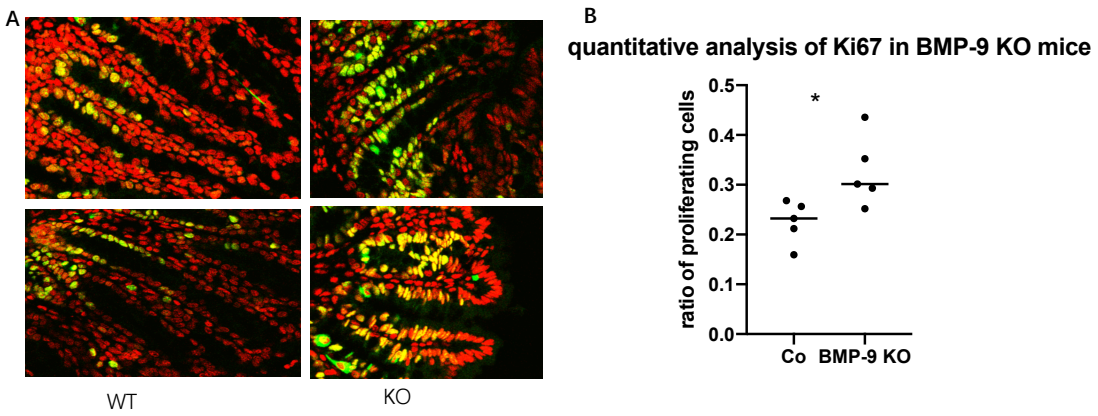

Fig. 12: IF staining of Ki67 in the intestine of BMP-9 Knockout mice. A) Wild-type (WT) and BMP-9 knock out (KO) mice (n=5 per group) were sacrificed and samples of the intestine were processed to paraffinblocks. IF stainings were performed against Ki67 (green color) and nuclei were counter-stained with Draq5(red color). B) Stainings were imaged using confocal microscopy and Image J was used for quantification. *$p<0.05$ as determined by t-test

7.6 BMP-9 supports a high ratio of ID1/Noggin, which predicts better patient survival

7.6.1 BMP-9 induces ID1 expression in N- and T-Orgs

Since ID1 expression was correlating with better patient survival (Fig. 3), we took a closer look at the ID1 expression level in N- and T-Orgs. With statistical significance, the array data showed that BMP-9 stimulates and Noggin reduces ID1 expression in both N- and T-Orgs. And this BMP-9 effect was not blocked by Noggin (Fig. 13A), indicating that Noggin does not inhibit BMP-9. Similar results were observed by real-time PCR analyses (Suppl. Fig. 10).

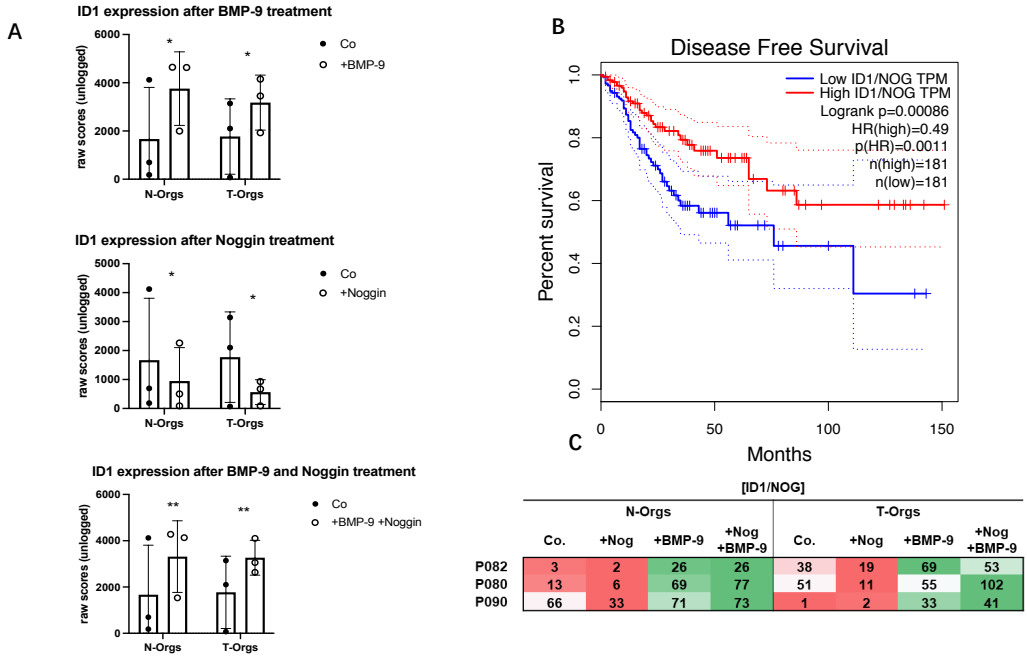

Fig. 13: Noggin reduces and BMP-9 enhances ID1 expression in Organoids and high ID1 in combination with low Noggin expression significantly correlates with better survival of CRC patients. A) Organoids were derived from human biopsies of normal and cancerous gut mucosa as depicted in figure 5 followed by in vitro stimulation with either recombinant Noggin (100 ng/ml) or BMP-9 (5 ng/ml) or both together. After 72 h RNA was isolated and processed for Affimetrix array analyses. The raw scores (unlogged values) for the individual ID1 expression in each sample (N as well as T of each patient's organoids) are plotted and values of untreated (Co.) are compared to either BMP-9-treated (+BMP-9), Noggin-treated (+Noggin) or treated with both (+BMP-9 +Noggin). For statistics, all 3 controls were compared to all 3 treated samples and significance was calculated using the unpaired t-test. *=p>0.05. B) Graphic depictions of the prognostic values of the mRNA levels of the ID1-to-Noggin ration in CRC patients from the TCGA-COAD+READ cohort analysed by GEPIA. High ID1/NOG expression levels significantly correlate with better disease free survival of the patients. C) Calculation of the ratio between ID1 and NOG in each patient's organoid sample using the array data depicted in A). Red: reduced ratio; Green: enhanced ratio.

7.6.2 P090 is associated with a worse patient outcome and low levels of ID1 expression

Our Patient 090 who expressed low levels of ID1 had both liver and lung metastasis (Table 2) which fits to the in silico data predictions (Fig. 3). As we just presented above, BMP-9 and Noggin regulate ID1 to an opposite direction, this leads to the hypothesis that BMP-9 may regulate the ID1/Noggin ratio and might thereby exert its anti-stem cell proliferation and anti-tumour effects in the colon. We additionally constructed a protein-protein interaction network based on functional enrichment analyses from String and found a close connection between BMP-9, ID1, Noggin, Lgr5 (a stem-cell marker) and Ki67 (Fig. 14).

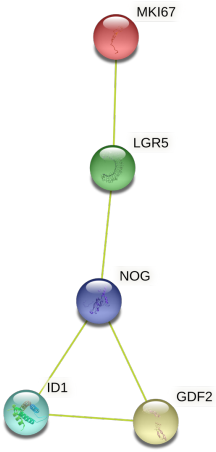

Fig. 14: Protein-protein interaction network analysis for the interactions between BMP-9, ID1, Noggin, Lgr5 and Ki67. The String Database was used for network analysis between the following proteins: BMP-9, ID1, Noggin, Lgr5 and Ki67. PPI enrichment p-value: 3.64e-07.

7.6.3 Higher ratio of ID1/Noggin predicts a better patient survival in colorectal cancer

We then went back to the in silico database GEPIA to investigate the correlation between the ID1/Noggin ratio and the disease-free survival times of the patients. Using the data from 362 patient samples we found that a high ratio of ID1/Noggin significantly correlates with better patient survival (P value: 0.00086; Fig. 13B).

7.6.4 BMP-9 supports a high ratio of ID1/Noggin

To further support our hypothesis that BMP-9 might mediate a better patient survival through the regulation of the ID1/Noggin ratio, we directly compared this ratio in samples of BMP-9 stimulated Organoids. A strong up-regulation of the ID1/Noggin ratio was found in BMP-9 stimulated Organoids of all three patients and Noggin was not able to inhibit this effect (Fig. 13C).

In summary, BMP-9 showed an anti-proliferative, tumour-suppressive effect most likely via up-regulating the ratio of ID1/Noggin leading to an improved disease-free survival time of the patients. Thereby BMP-9 could be a promising new therapy factor for CRC patients. Even in organoids from our patient 090, who had a very low basic ID1/Noggin ratio, BMP-9 was able to enhance this ratio (Fig. 13C).

7.7 T-Organoids instruct adjacent cancer associated fibroblasts (CAFs) to up-regulate ID's, Noggin and immune-modulators like IL-6

7.7.1 Modelling the tumour-stroma interactions through CAFs and tumour Organoids co-culture

Cancer associated fibroblasts (CAFs) have been reported to represent important modulators of colorectal cancer growth and metastases formation[66, 67]. However, CAFs are a very heterogeneous cell population[68, 69] and individual differences from one patient to the next can be expected. We therefore used a model where CAFs from the same patient (n=3) are isolated at the same time as the T-Orgs are being generated. With this model of tumour-stroma cross-talk, we again performed microarray analyses of all four conditions: CAFs cultured alone or in transwell co-culture with their corresponding T-Orgs (without direct cell-to-cell contact) as well as T-Orgs alone or after co-culture with their corresponding CAFs (Fig 15).

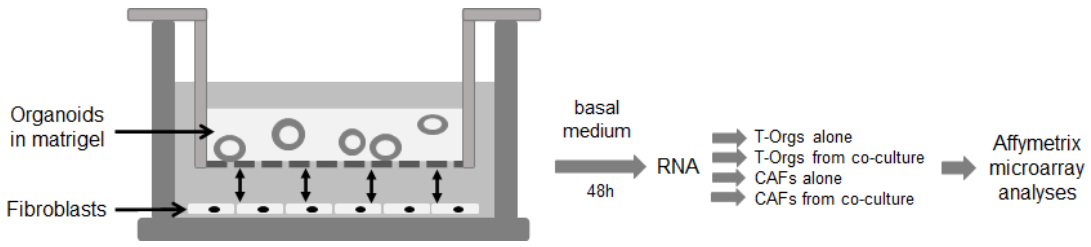

Fig. 15: Experimental setup of co-culture experiments of T-Orgs with CAFs. For co-culture experiments of T-Orgs with cancer associated fibroblasts (CAFs), half of the fresh tumour biopsies (from 3 individual patients) were processed for Organoid generation as described in Fig. 5 and were established for 24h (in ENA) in transwell inserts. The other half was used to obtain fibroblast lines by outgrowth (in DMEM). When inserts were combined with the established fibroblast monolayer, the medium was changed to advanced medium. RNA was obtained after 48h and processed for micro array analyses. The arrow indicates that through the membrane of the insert T-Orgs and CAFs are allowed to communicate with each other via secreted factors.

When analysing the resulting expression data by microarray, we first focussed on changes in expression of genes that might be directly related to the BMP-9 signalling pathway. We found that the co-culture condition generally led to upregulation of IDs in CAFs from all three patients (Fig. 16A). The inducing signal (most likely BMPs) can be initiated by secreted cytokines from the T-Orgs or by simultaneous upregulation of such cytokines in CAFs themselves. And indeed, some BMPs, including BMP-9 (Gdf2) are slightly, but not significantly, upregulated in CAFs by co-culture (Fig. 16A). Among the group of BMP-signalling modulators we found that Noggin was also significantly upregulated in CAF's by co-culture (Fig. 16A), whereas the BMP-receptors were not significantly changed (Suppl. Fig. 11). Although there was similar ALK1 expression in T-Orgs and CAFs (Suppl. Fig. 12), in the Organoids no significant changes of IDs or BMPs were observed upon co-culture and no enhanced BMP-signalling was taking place (data not shown).

A

	P018		P055		P080			
	basal	co-culture	basal	co-culture	basal	co-culture	logFC	P.Value
BMP2	8,79	8,82	8,48	9,64	7,16	6,98	0,34	0,6310
BMP3	5,13	4,94	5,15	4,62	5,01	4,86	-0,29	0,1257
BMP6	5,84	6,09	6,43	7,35	5,16	5,17	0,39	0,4328
GDF2 (=BMP-9)	5,07	5,29	5,25	5,42	5,14	5,32	0,19	0,2305
BMP10	3,66	4,01	4,28	3,49	4,14	3,51	-0,35	0,1271
BMP15	4,94	4,67	4,66	4,27	4,74	4,64	-0,25	0,1307
NOG	5,86	6,57	5,86	6,31	5,77	6,51	0,64	0,0008 *
ID1	5,58	7,14	6,65	7,45	6,04	7,72	1,35	0,0048 *
ID2	7,98	8,93	8,46	9,21	8,12	8,84	0,80	0,0031 *
ID3	8,36	9,12	8,09	9,26	7,00	8,53	1,15	0,0088 *
ID4	6,66	7,41	7,18	7,41	7,60	8,00	0,46	0,0796

higher expressed
no change
lower expressed

B

	P018		P055		P080			
	basal	co-culture	basal	co-culture	basal	co-culture	logFC	P.Value
IL6	6,72	8,35	5,02	9,18	5,50	8,75	3,01	0,0000 *
IL1B	5,48	6,79	4,71	5,86	3,75	4,76	1,16	0,1599
TNF	5,78	6,36	5,69	6,33	6,12	5,95	0,35	0,1653
CXCL8	5,74	7,04	6,54	11,23	5,61	7,57	2,65	0,0205 *
CXCL6	7,21	8,19	7,28	10,03	6,82	6,99	1,30	0,0417 *
CXCL2	7,42	7,76	7,46	7,85	7,12	7,43	0,35	0,0955
CXCL1	8,15	9,32	8,99	10,29	5,97	6,90	1,14	0,2459
CCL2	9,45	10,84	11,11	12,09	11,02	11,90	1,08	0,0373 *

higher expressed
no change
lower expressed

Fig. 16: IDs, Noggin and immune-modulatory genes are induced in CAFs by co-culture with T-Orgs. A) Expression of BMPs and their classical target genes, the ID-proteins, were determined in CAFs of each patient (P018, P055 and P080) as basal expression compared to co-culture with their corresponding T-Orgs. B) Expression of a selection of genes related to inflammatory and immune-regulatory factors is enhanced in CAFs upon co-culture with their corresponding T-Orgs. Expression levels that were enhanced by co-culture are shown in green, those reduced in red and unchanged in yellow. logFC: average fold change (log data) of all three patients. (*): statistically significant change ($p<0.05$).

7.7.2 CAFs express higher levels of immune modulators in co-culture with tumour Organoids

Interestingly, one of the most significantly induced genes in co-cultured CAFs was IL-6, a cytokine that we previously described to directly induce BMP-9 expression in liver myofibroblasts[70]. Several other immune-modulatory genes like CXCL8, CXCL6 and CCl2 were significantly induced as well (Fig. 16B) indicating that the T-Orgs secrete factors that affect production of inflammatory mediators in adjacent CAFs.

8 Discussion

BMP-9 is a protein encoded by the GDF2 gene. It belongs to the TGF-β family and contains a C-terminal TGF-β superfamily domain and an N-terminal prodomain. By binding to its high affinity receptor ALK1, SMAD1, 5, 8 proteins get phosphorylated and transfered into the nucleus where they activate transcription of target genes like the ID proteins. BMP-9 is quite unique compared to other BMPs: for example, BMP-9 can form stable dimers in two different ways, the D-form and the M-form. In the M- but not the D-form there are no intermolecular disulfide bonds. No matter if an intermolecular disulphide bond exists or not, BMP-9 can form stable dimers and it cannot be inhibited by Noggin and BMP3[71] . BMP-9 is mainly expressed in the liver, which we also showed using human and murine liver and colon tissue samples (Fig. 4). It is secreted in an active form into the circulation and functions on different organs. Via the co-receptor endoglin, BMP-9 plays an important role in angiogenesis and blood vessel homeostasis[72-74]. BMP-9 was found to be able to reduce blood glucose levels in diabetic mice[75]. Regarding BMP-9's function in fibrosis and cancer, reports were rather controversial. There does not exist much research regarding BMP-9's function in colorectal cancer, nevertheless, opposite views were presented from three different groups: in contrast to our in silico data derived from GENT, Fan et al. reported that the expression level of BMP-9 was gradually increased with the change of normal mucosa towards adenoma and adenocarcinoma formation. In addition, a high level of BMP-9 expression goes along with a worse patients' overall survival[76]. In line with our results, two other groups are supporting the hypothesis that BMP-9 acts rather tumour-suppressive[77, 78].

Pioneer work regarding the generation of gut Organoids was published by Sato. et al. [46, 51]. We followed this established method and compared Organoids derived from normal and tumour tissues from the same patients. To maintain stemness, the WNT activator R-Spondin and Wnt3A together with the BMP antagonist Noggin are typically added to Organoids culture medium[46, 52]. Taking into account that in addition to Wnt, R-Spondin, EGF and Noggin the "normal" Organoid growth media (ENA and WENRA) contain many additional factors and other inhibitors (listed in table 3) that might directly or indirectly affect or interfere with BMP-9 signalling, we used for our

experiments only Advanced medium without any factors. If we artificially block certain pathways (e.g. Noggin inhibits BMP-2 signalling but also that of certain other BMPs) and then stimulate with BMP-9, we will never know if the response was simply an artificial result of blocking the other pathway(s) in parallel. For example, if there is ongoing BMPs activity, the endogenous levels of Smads might all be "in use" so that this indirectly might prevent BMP-9 from signaling in parallel. Since we cannot really know which TGFbeta's/BMP's (or others) are actively signaling in these Organoids (or in the corresponding in vivo situation) it seems logical to first withdraw all components from the medium that might interfere with BMP-9 signaling. Very similar to reducing the serum concentrations in cell culture experiments in order to "starve" the cells before the experiment. One concern under these circumstances is of course that this minimal medium might negatively affect the Organoids' survival ability. According to data from Wilson et. al. e.g. Wnt3A is an essential factor for growth and survival of Organoids for long term culture[79]. We therefore compared the Organoids morphology, viability, functionality and differentiation status when being cultured in Advanced medium compared to "normal" medium. We found that at least for 72 hours, both N- and T-Orgs showed no clear morphological or viability changes and they were still able to differentiate into other epithelial cell types. Nevertheless, they proliferated slower in Advanced medium. However, it is still difficult to state how close we can really get to the in vivo situation, because it is still not clear today how exactly Wnt, BMP and other factors/pathways are being regulated during the crypts to villi migration process of the intestinal cells.

Although gut Organoids were proven to be able to recapitulate certain patients' responses in the clinic[80], it is still important to further characterize them as compared to the in vivo situation. In our N-/T-Organoids, mainly differentiated epithelial cells were found and stromal cells like fibroblasts and endothelial cells were absent which indicates a high similarity between Organoids and the in vivo mucosa. However, the cellular cross-talk between the intestinal epithelium and the underlying tissue containing e.g. endothelial and fibroblastic cell types cannot be simulated by such Organoids.

In our tumour Organoids, gene sets related to cell cycle, proliferation, amino acid and lipid metabolism and damage response are highly enriched as compared to normal Organoids and immune response- as well as glycan biosynthesis pathways are enriched in normal Organoids. This fits also to the widely accepted characteristics of cancer tissue. Interestingly, enhanced glycolysis was not found in our tumour Organoids. The reason could be that glycolysis may be carried out by the tumour stromal compartment instead of the tumour cells themselves[81].

Colorectal cancer is a heterogeneous disease and thus there are many different ways of classifications based on mRNA expression profile analyses. Marisa et al. defined 6 different groups by consensus unsupervised analysis based on Gene Expression Profiles (GEP)[82]. Based on the expression profile of inflammatory genes, "Consensus Cluster Plus" was used for the classification of colorectal cancer molecular subtypes. Two clusters were identified, in which cluster 2 was associated with higher expression of MHC, higher score of tumourigenic cytokines, stemness scores and degree of immune cell infiltrates[83]. Consensus molecular subtypes (CMS) were defined to unite different kinds of subtyping schemes based on multiple independent subtyping classifications and was derived from analysing 18 data sets with n=4151 human samples[62]. There were four CMS groups defined: CMS1 presents with enriched immune infiltration signatures, in CMS2 Wnt and Myc pathways are activated, in CMS3 metabolic pathway genes are highly expressed and CMS4 shows an enrichment of epithelia-mesenchymal transition (EMT) genes expression. In general, CMS classification is also a strong prognostic factor for predicting the overall survival (OS) of the patients. CMS4 correlates with the worst OS, and is at the same time suitable for classification of colorectal adenomas[84]. Based on our Organoids' expression profiles, patient P080 belongs to CMS1, P082 fits to CMS3 and P090 belongs most likely to CMS4. Thereby our small cohort still covers a large range of possible CMS subtypes.

In our small tumour Organoids group, the BMP target genes ID1-4 were up-regulated in two patients as compared to the non-malignant tissue derived Organoids, while in the third patient they were down-regulated. Our finding that high Noggin expression seems to act tumour-promoting is well in line with previous findings[44]. Different from the commonly made conclusion that BMP-9 plays a pro-tumourigenic role in cancer[24-

[26], our gene set enrichment data support an anti-proliferative and tumour-suppressive function of BMP-9 in both N- and T-Organoids. Ki67 which is not only a proliferation marker, but also a promising prognostic predictor[85, 86], was reduced in BMP-9 treated T-Organoids and Noggin was not able to inhibit this BMP-9 effect. Accordingly, in the stem cell/ transient amplifying area of the intestinal epithelium from BMP-9 knock out mice, we found more Ki67 positive cells than in the wild-type controls. Supporting the conclusion that BMP-9 exerts such anti-proliferative function not only in vitro but also in vivo (at least in mice). This is also an interesting new finding, because it is believed that stem cells usually need factors of the stem cell niche, especially interaction with fibroblast-derived factors like WNT, BMPs and HGF for proliferation and differentiation. It seems that BMP-9 can act anti-proliferative even without the full interaction with the stem cell niche. Possibly the high expression of the BMP-9 receptor ALK1 in colonic- or cancer-stem cells that we found mediates this effect. Further experiments using IF or flow cytometry would be very helpful to better understand this mechanism.

ID1 and Noggin were both previously reported to promote tumour growth. In this context, ID1 acts mainly through its effect on tumour angiogenesis, but its role in colon cancer stem cells is actually not clear. Noggin in turn owns its pro-cancer effects to the ability to inhibit several BMPs (BMP2/4/6/7)[39]. This led us to the hypothesis that BMP-9 might inhibit tumourigenesis by regulating the ID1/Noggin ratio. We indeed found an up-regulated ID1/Noggin ratio after BMP-9 stimulation. The proposed concept is that reduced Noggin exerts reduced inhibition of the other BMPs' pro-differentiation function (levels of ID expression can rise) in combination with BMP-9s' anti-proliferative function on colon stem cells leading to a higher degree of cells differentiation instead of self-replication.

We further found that co-culturing T-Orgs with their corresponding CAFs stimulated expression of immune-modulatory factors like IL-6 in the fibroblasts. We described earlier that IL-6 in turn can directly upregulate BMP-9 expression in liver fibroblasts[70]. In line with this, co-culture not only led to up-regulated expression of ID's, but it also led to slightly enhanced expression of BMP-9 itself in the CAFs, but not in the Organoids. This upregulation of BMP-9 expression was rather small, but very

consistent for all three patients (Fig. 16A) and might represent the result of local IL-6 induction. Taking the findings of Fan et al. into account, who described an enhanced local expression of BMP-9 in colorectal cancer patient samples[76], together with our finding of high ALK1 expression in the gut in general (Fig. 4), this stromal BMP-9 induction might be of high relevance. In any case it should be discriminated between levels of BMP-9 in the blood, that are most likely liver-derived, and levels of local expression (e.g. in local fibroblasts). In the case of CRC-patients it is yet not investigated if there is any correlation between the serum-levels of BMP-9 protein and disease progression or outcome. However, besides ID's we also found a significant upregulation of Noggin in the co-cultured CAF's. We found an interesting relation between Noggin down-regulating ID1 in Organoids and BMP-9 (as expected) upregulating it and being unaffected by the presence of Noggin (Fig. 13A). This led to our concept that Noggin should be tumour-promoting while ID1 should be tumour-suppressive. In favour of this concept we found a significant correlation between high Noggin expression and reduced patient survival times and an even more significant correlation between the combination of high ID1 and low Noggin with increased survival time (Fig. 13B).

Overall, our co-culture data point to the conclusion that T-Orgs secrete molecules that induce immune-modulatory factors like IL-6 in CAFs and that this is accompanied by enhanced ID1 as well as Noggin expression in the CAF's (see scheme in Fig. 17). Although there is similar ALK1 expression in T-Orgs and CAFs (Suppl. Fig. 12), no enhanced BMP-signalling (or IL-6 expression) is taking place in the Organoids in co-culture. In this situation high levels of BMP-9 (e.g. applied therapeutically) would possibly support ID1 expression even in the presence of Noggin and would thereby possibly act tumour-suppressive in vivo.

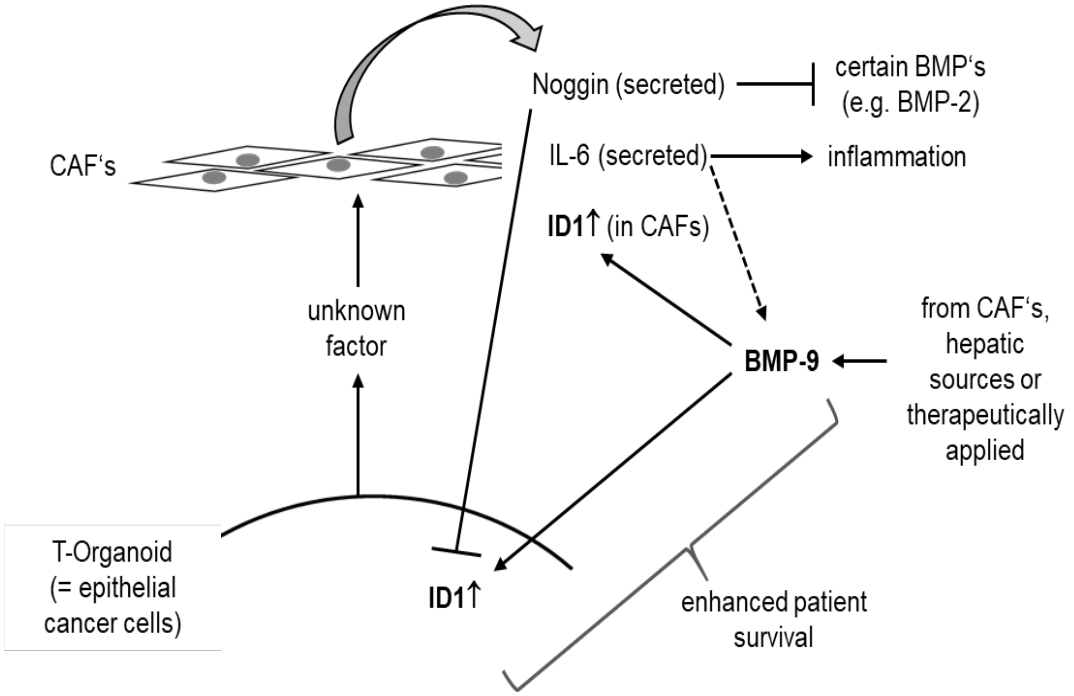

Fig. 17: Scheme summarizing how BMP-9 acts tumour-suppressive by supporting ID1 induction with existence of CAFs even in the situation of high presence of Noggin. The epithelial cancer cells secrete so far undefined factors that instruct the surrounding fibroblasts (cancer associated fibroblasts, CAF's) to upregulate their expression of Noggin, IL-6 and ID1. Noggin, being secreted can then act on the tumour cells to reduce ID1 expression (see Fig. 13A) either by itself or indirectly via inhibition of Noggin-sensitive BMP's like BMP-2. IL-6 plays an important role in inflammation but was also described to directly induce BMP-9, at least in liver myofibroblasts. BMP-9, derived from CAF's, the liver or given therapeutically would support high ID1 levels in CAF's as well as tumour cells and is not inhibited by Noggin (see fig. 13A). Thereby BMP-9 would enhance ID1 expression which leads to better survival of CRC-patients (see Fig. 3A).

9. Summary

CRC is one of the most lethal tumours and for later disease stage patients, promising therapy is still missing. The role of BMP-9 in tumourigenesis in general is quite controversial, although there were few indirect researches supporting a protective effect of BMP-9 in CRC. We investigated BMP-9s' functions in CRC and its underlying mechanisms. Using N- and T- paired patients' 3D Organoids as models and BMP-9 knockout mice samples we investigated the direct effect of BMP-9 on the intestinal epithelium. Before BMP-9 application, we first established the colon Organoids model. Though 3D Organoids can better mimic the in vivo situation than regular monolyer culture, the possible influence of the complex culture medium on signalling pathways of the TGF-β family of cytokines was not clear. Therefore, in our stimulation/co-culture experiments, only Advanced medium was used containg a strongly reduced number of factors. The Organoids' morphology and viability using this medium were controlled before starting the experiments. In order to better characterize the model, we analysed the cell types, cell characteristics and CMS subgroups of our Organoids. In silico data from GENT, STRING and GEPIA and TCGA-COAD+READ cohorts, showed an adjustability of BMP-9 signaling in Organoids and basal expression level of the BMP-9 signaling pathway components were used for predictions. BMP-9s' anti-proliferation effects were proven by: 1. Enriched gene sets for proliferation in non-BMP-9 treated organoids; 2. Reduced Ki67 expression in BMP-9 treated Organoids and 3. Inhibited proliferation in the stem cell/TA zone of the colon epithelium in BMP-9 KO mice. The mechanism of BMP-9s' anti-proliferation/tumourigenesis activity was explored through: 1. In silico data, showing that an increased ID1/Noggin ratio is associated with longer patient disease free survival times; 2. An increased ratio of ID1/Noggin after BMP-9 stimulation and 3. Up-regulated expression of ID1 in CAFs in the presence of BMP-9.

In summary, our data confirm that patient-derived Organoids from normal and matched tumour-biopsies represent highly suitable models to study individual responses and therefore such Organoids will most likely further advance personalized medicine approaches in the future. BMP-9 profoundly affects the normal as well as the malignant gut mucosa and these effects, including up-regulation of the ratio of ID1/Noggin, are

supposedly tumour-suppressive, implying that BMP-9 mimetics might represent promising tools for future therapy approaches against initiation and progression of CRC in patients.

10. References

1. Xi Y, Xu P. Global colorectal cancer burden in 2020 and projections to 2040. Transl Oncol. 2021;14: 101174.

2. Krebs in Deutschland für 2015/2016 Zentrum für Krebsregisterdaten. 19.12.2019.

3. Lewandowska A, Rudzki G, Lewandowski T, Stryjkowska-Gora A, Rudzki S. Title: Risk Factors for the Diagnosis of Colorectal Cancer. Cancer Control. 2022;29: 10732748211056692.

4. Conteduca V, Sansonno D, Russi S, Dammacco F. Precancerous colorectal lesions (Review). Int J Oncol. 2013;43: 973-984.

5. Williams CD, Grady WM, Zullig LL. Use of NCCN Guidelines, Other Guidelines, and Biomarkers for Colorectal Cancer Screening. J Natl Compr Canc Netw. 2016;14: 1479-1485.

6. Venugopal A, Carethers JM. Epidemiology and biology of early onset colorectal cancer. EXCLI J. 2022;21: 162-182.

7. Gehart H, Clevers H. Tales from the crypt: new insights into intestinal stem cells. Nat Rev Gastroenterol Hepatol. 2019;16: 19-34.

8. Baker AM, Cereser B, Melton S, et al. Quantification of crypt and stem cell evolution in the normal and neoplastic human colon. Cell Rep. 2014;8: 940-947.

9. Nooteboom M, Johnson R, Taylor RW, et al. Age-associated mitochondrial DNA mutations lead to small but significant changes in cell proliferation and apoptosis in human colonic crypts. Aging Cell. 2010;9: 96-99.

10. Potten CS, Gandara R, Mahida YR, Loeffler M, Wright NA. The stem cells of small intestinal crypts: where are they? Cell Prolif. 2009;42: 731-750.

11. Ponz de Leon M, Di Gregorio C. Pathology of colorectal cancer. Dig Liver Dis. 2001;33: 372-388.

12. Wu X, Lin H, Li S. Prognoses of different pathological subtypes of colorectal cancer at different stages: A population-based retrospective cohort study. BMC Gastroenterol. 2019;19: 164.

13. Armaghany T, Wilson JD, Chu Q, Mills G. Genetic alterations in colorectal cancer. Gastrointest Cancer Res. 2012;5: 19-27.

14. Harada S, Morlote D. Molecular Pathology of Colorectal Cancer. Adv Anat Pathol. 2020;27: 20-26.

15. Hashiguchi Y, Muro K, Saito Y, et al. Japanese Society for Cancer of the Colon and Rectum (JSCCR) guidelines 2019 for the treatment of colorectal cancer. Int J Clin Oncol. 2020;25: 1-42.
16. Nikbakht HA, Hassanipour S, Shojaie L, et al. Survival Rate of Colorectal Cancer in Eastern Mediterranean Region Countries: A Systematic Review and Meta-Analysis. Cancer Control. 2020;27: 1073274820964146.
17. Wozney JM, Rosen V, Celeste AJ, et al. Novel regulators of bone formation: molecular clones and activities. Science. 1988;242: 1528-1534.
18. Song Q, Zhong L, Chen C, et al. miR-21 synergizes with BMP9 in osteogenic differentiation by activating the BMP9/Smad signaling pathway in murine multilineage cells. Int J Mol Med. 2015;36: 1497-1506.
19. Chen Y, Ma B, Wang X, et al. Potential Functions of the BMP Family in Bone, Obesity, and Glucose Metabolism. J Diabetes Res. 2021;2021: 6707464.
20. Li W, Long L, Yang X, et al. Circulating BMP9 Protects the Pulmonary Endothelium during Inflammation-induced Lung Injury in Mice. Am J Respir Crit Care Med. 2021;203: 1419-1430.
21. West J. BMP9 in Acute Respiratory Distress Syndrome: Decades of BMP Studies in Vascular Biology Paying Off? Am J Respir Crit Care Med. 2021;203: 1341-1342.
22. Desroches-Castan A, Tillet E, Ricard N, et al. Bone Morphogenetic Protein 9 Is a Paracrine Factor Controlling Liver Sinusoidal Endothelial Cell Fenestration and Protecting Against Hepatic Fibrosis. Hepatology. 2019;70: 1392-1408.
23. Breitkopf-Heinlein K, Meyer C, König C, et al. BMP-9 interferes with liver regeneration and promotes liver fibrosis. Gut. 2017;66: 939-954.
24. Chen H, Nio K, Tang H, et al. BMP9-ID1 Signaling Activates HIF-1alpha and VEGFA Expression to Promote Tumor Angiogenesis in Hepatocellular Carcinoma. Int J Mol Sci. 2022;23.
25. Jung JW, Yoon SM, Kim S, et al. Bone morphogenetic protein-9 is a potent growth inhibitor of hepatocellular carcinoma and reduces the liver cancer stem cells population. Oncotarget. 2016;7: 73754-73768.
26. Cai C, Itzel T, Gaitantzi H, et al. Identification of liver-derived bone morphogenetic protein (BMP)-9 as a potential new candidate for treatment of colorectal cancer. J Cell Mol Med. 2022;26: 343-353.

27. Jiang QQ, Liu BB, Xu KS. New insights into BMP9 signaling in liver diseases. Mol Cell Biochem. 2021;476: 3591-3600.
28. Herrera B, Dooley S, Breitkopf-Heinlein K. Potential roles of bone morphogenetic protein (BMP)-9 in human liver diseases. Int J Mol Sci. 2014;15: 5199-5220.
29. Bi J, Ge S. Potential roles of BMP9 in liver fibrosis. Int J Mol Sci. 2014;15: 20656-20667.
30. Breitkopf-Heinlein K, Meyer C, Konig C, et al. BMP-9 interferes with liver regeneration and promotes liver fibrosis. Gut. 2017;66: 939-954.
31. Ghil SH, Jeon YJ, Suh-Kim H. Inhibition of BETA2/NeuroD by Id2. Exp Mol Med. 2002;34: 367-373.
32. Trausch-Azar JS, Lingbeck J, Ciechanover A, Schwartz AL. Ubiquitin-Proteasome-mediated degradation of Id1 is modulated by MyoD. J Biol Chem. 2004;279: 32614-32619.
33. Roschger C, Cabrele C. The Id-protein family in developmental and cancer-associated pathways. Cell Commun Signal. 2017;15: 7.
34. Ding Y, Wang G, Ling MT, et al. Significance of Id-1 up-regulation and its association with EGFR in bladder cancer cell invasion. Int J Oncol. 2006;28: 847-854.
35. Zhao Z, Bo Z, Gong W, Guo Y. Inhibitor of Differentiation 1 (Id1) in Cancer and Cancer Therapy. Int J Med Sci. 2020;17: 995-1005.
36. Yang Y, Wang HC, Sun XH. Id1 induces apoptosis through inhibition of RORgammat expression. BMC Immunol. 2008;9: 20.
37. Miyazono K, Miyazawa K. Id: a target of BMP signaling. Sci STKE. 2002;2002: pe40.
38. Ma J, Sanchez-Duffhues G, Goumans MJ, Ten Dijke P. TGF-beta-Induced Endothelial to Mesenchymal Transition in Disease and Tissue Engineering. Front Cell Dev Biol. 2020;8: 260.
39. Rosen V. BMP and BMP inhibitors in bone. Ann N Y Acad Sci. 2006;1068: 19-25.
40. Diaz-Moreno M, Armenteros T, Gradari S, et al. Noggin rescues age-related stem cell loss in the brain of senescent mice with neurodegenerative pathology. Proc Natl Acad Sci U S A. 2018;115: 11625-11630.
41. Chien SY, Tsai CH, Liu SC, et al. Noggin Inhibits IL-1beta and BMP-2 Expression, and Attenuates Cartilage Degeneration and Subchondral Bone Destruction in Experimental Osteoarthritis. Cells. 2020;9.

42. Kang HW, Walvick R, Bogdanov A, Jr. In vitro and In vivo imaging of antivasculogenesis induced by Noggin protein expression in human venous endothelial cells. FASEB J. 2009;23: 4126-4134.
43. Sawant A, Chanda D, Isayeva T, Tsuladze G, Garvey WT, Ponnazhagan S. Noggin is novel inducer of mesenchymal stem cell adipogenesis: implications for bone health and obesity. J Biol Chem. 2012;287: 12241-12249.
44. Sun Z, Gao X, Zabkiewicz C, et al. Noggin is associated with a poor prognosis of gastric cancer by promoting the proliferation of gastric cancer cells via the upregulation of EGFR. Int J Oncol. 2020;57: 813-824.
45. Smith E, Cochrane WJ. CYSTIC ORGANOID TERATOMA: (Report of a Case). Can Med Assoc J. 1946;55: 151-152.
46. Sato T, Stange DE, Ferrante M, et al. Long-term expansion of epithelial organoids from human colon, adenoma, adenocarcinoma, and Barrett's epithelium. Gastroenterology. 2011;141: 1762-1772.
47. Boj SF, Hwang CI, Baker LA, et al. Organoid models of human and mouse ductal pancreatic cancer. Cell. 2015;160: 324-338.
48. Broutier L, Mastrogiovanni G, Verstegen MM, et al. Human primary liver cancer-derived organoid cultures for disease modeling and drug screening. Nat Med. 2017;23: 1424-1435.
49. Choi SH, Kim YH, Hebisch M, et al. A three-dimensional human neural cell culture model of Alzheimer's disease. Nature. 2014;515: 274-278.
50. Tang XY, Wu S, Wang D, et al. Human organoids in basic research and clinical applications. Signal Transduct Target Ther. 2022;7: 168.
51. Sato T, Vries RG, Snippert HJ, et al. Single Lgr5 stem cells build crypt-villus structures in vitro without a mesenchymal niche. Nature. 2009;459: 262-265.
52. Barbachano A, Fernandez-Barral A, Bustamante-Madrid P, et al. Organoids and Colorectal Cancer. Cancers (Basel). 2021;13.
53. Zarin B, Rafiee L, Daneshpajouhnejad P, Haghjooy Javanmard S. A review on the role of CAFs and CAF-derived exosomes in progression and metastasis of digestive system cancers. Tumour Biol. 2021;43: 141-157.
54. Wanandi SI, Ningsih SS, Asikin H, Hosea R, Neolaka GMG. Metabolic Interplay between Tumour Cells and Cancer-Associated Fibroblasts (CAFs) under Hypoxia versus Normoxia. Malays J Med Sci. 2018;25: 7-16.

55. Hurtado P, Martinez-Pena I, Pineiro R. Dangerous Liaisons: Circulating Tumor Cells (CTCs) and Cancer-Associated Fibroblasts (CAFs). Cancers (Basel). 2020;12.
56. Monteran L, Erez N. The Dark Side of Fibroblasts: Cancer-Associated Fibroblasts as Mediators of Immunosuppression in the Tumor Microenvironment. Front Immunol. 2019;10: 1835.
57. Ozdemir BC, Pentcheva-Hoang T, Carstens JL, et al. Depletion of carcinoma-associated fibroblasts and fibrosis induces immunosuppression and accelerates pancreas cancer with reduced survival. Cancer Cell. 2014;25: 719-734.
58. Biffi G, Tuveson DA. Diversity and Biology of Cancer-Associated Fibroblasts. Physiol Rev. 2021;101: 147-176.
59. Zhan T, Belle S, Valentini E, et al. Cancer-Associated Mutations in Normal Colorectal Mucosa Adjacent to Sporadic Neoplasia. Clin Transl Gastroenterol. 2020;11: e00212.
60. Eide PW, Bruun J, Lothe RA, Sveen A. CMScaller: an R package for consensus molecular subtyping of colorectal cancer pre-clinical models. Sci Rep. 2017;7: 16618.
61. Chang C. Agonists and Antagonists of TGF-beta Family Ligands. Cold Spring Harb Perspect Biol. 2016;8.
62. Guinney J, Dienstmann R, Wang X, et al. The consensus molecular subtypes of colorectal cancer. Nat Med. 2015;21: 1350-1356.
63. Smeby J, Sveen A, Bergsland CH, et al. Exploratory analyses of consensus molecular subtype-dependent associations of TP53 mutations with immunomodulation and prognosis in colorectal cancer. ESMO Open. 2019;4: e000523.
64. Wang X. Identification of common tumor signatures based on gene set enrichment analysis. In Silico Biol. 2011;11: 1-10.
65. Laczmanska I, Sasiadek MM. Tyrosine phosphatases as a superfamily of tumor suppressors in colorectal cancer. Acta Biochim Pol. 2011;58: 467-470.
66. Isella C, Terrasi A, Bellomo SE, et al. Corrigendum: Stromal contribution to the colorectal cancer transcriptome. Nat Genet. 2016;48: 1296.
67. Kalluri R. The biology and function of fibroblasts in cancer. Nat Rev Cancer. 2016;16: 582-598.
68. Kobayashi H, Enomoto A, Woods SL, Burt AD, Takahashi M, Worthley DL. Cancer-associated fibroblasts in gastrointestinal cancer. Nat Rev Gastroenterol Hepatol. 2019;16: 282-295.

69. Stzepourginski I, Nigro G, Jacob JM, et al. CD34+ mesenchymal cells are a major component of the intestinal stem cells niche at homeostasis and after injury. Proc Natl Acad Sci U S A. 2017;114: E506-e513.
70. Gaitantzi H, Karch J, Germann L, et al. BMP-9 Modulates the Hepatic Responses to LPS. Cells. 2020;9.
71. Kopsachilis N, Carifi G, Cunningham C. Rapid exaggeration of a pre-existing epiretinal membrane following uneventful cataract surgery. Clin Exp Optom. 2015;98: 94-96.
72. Redgrave RE, Tual-Chalot S, Davison BJ, et al. Cardiosphere-Derived Cells Require Endoglin for Paracrine-Mediated Angiogenesis. Stem Cell Reports. 2017;8: 1287-1298.
73. Saito T, Bokhove M, Croci R, et al. Structural Basis of the Human Endoglin-BMP9 Interaction: Insights into BMP Signaling and HHT1. Cell Rep. 2017;19: 1917-1928.
74. Franco CA, Gerhardt H. Blood flow boosts BMP signaling to keep vessels in shape. J Cell Biol. 2016;214: 793-795.
75. Chen C, Grzegorzewski KJ, Barash S, et al. An integrated functional genomics screening program reveals a role for BMP-9 in glucose homeostasis. Nat Biotechnol. 2003;21: 294-301.
76. Fan Y, Guo L, Zheng H, Ji C, Wang W, Sun H. BMP-9 is a novel marker for colorectal tumorigenesis undergoing the normal mucosa-adenoma-adenocarcinoma sequence and is associated with colorectal cancer prognosis. Oncol Lett. 2020;19: 271-282.
77. Li FS, Huang J, Cui MZ, et al. BMP9 mediates the anticancer activity of evodiamine through HIF1alpha/p53 in human colon cancer cells. Oncol Rep. 2020;43: 415-426.
78. Yuan SX, Wang DX, Wu QX, et al. BMP9/p38 MAPK is essential for the antiproliferative effect of resveratrol on human colon cancer. Oncol Rep. 2016;35: 939-947.
79. Wilson SS, Mayo M, Melim T, et al. Optimized Culture Conditions for Improved Growth and Functional Differentiation of Mouse and Human Colon Organoids. Front Immunol. 2020;11: 547102.
80. Granat LM, Kambhampati O, Klosek S, Niedzwecki B, Parsa K, Zhang D. The promises and challenges of patient-derived tumor organoids in drug development and precision oncology. Animal Model Exp Med. 2019;2: 150-161.

81. Pavlides S, Whitaker-Menezes D, Castello-Cros R, et al. The reverse Warburg effect: aerobic glycolysis in cancer associated fibroblasts and the tumor stroma. Cell Cycle. 2009;8: 3984-4001.
82. Marisa L, de Reynies A, Duval A, et al. Gene expression classification of colon cancer into molecular subtypes: characterization, validation, and prognostic value. PLoS Med. 2013;10: e1001453.
83. Qiu C, Shi W, Wu H, et al. Identification of Molecular Subtypes and a Prognostic Signature Based on Inflammation-Related Genes in Colon Adenocarcinoma. Front Immunol. 2021;12: 769685.
84. Komor MA, Bosch LJ, Bounova G, et al. Consensus molecular subtype classification of colorectal adenomas. J Pathol. 2018;246: 266-276.
85. Nagahama A, Yashiro M, Kawashima T, et al. Combination of p53 and Ki67 as a Promising Predictor of Postoperative Recurrence of Meningioma. Anticancer Res. 2021;41: 203-210.
86. Kaya R, Takanashi H, Nakajima A, et al. Prognostic significance of Ki67 during neoadjuvant chemotherapy in primary unresectable ovarian cancer. J Obstet Gynaecol Res. 2021;47: 3979-3989.
87. Farin HF, Van Es JH, Clevers H. Redundant sources of Wnt regulate intestinal stem cells and promote formation of Paneth cells. Gastroenterology. 2012;143: 1518-1529.e1517.

11. Own publications

(8) *Presence of ALK1 determines the switch from anti- tumorigenic to pro-tumorigenic BMP-9 signalling in hepatocellular carcinoma (HCC).* Joaquín Araos*, **Chen Cai***, Haristi Gaitantzi, Timo Itzel, Andreas Teufel, Qi Li, Keshu Xu, Honglei Weng, Steven Dooley, Lukas J A C Hawinkels, Emrullah Birgin, Nuh Rahbari, Matthias P Ebert, and Katja Breitkopf-Heinlein. (*shared first authorship), manuscript in preparation.

(7) I*ntestinal BMP-9 locally upregulates FGF19 and is down-regulated in obese patients with diabetes.*Stephan Drexler 1, **Chen Cai** 1, Anna-Lena Hartmann 2, Denise Moch 2, Haristi Gaitantzi 2, Theresa Ney 2, Yuwei Zheng 2, Mohammad Rahbari 3, Annalena Treffs 2, Alena Reiser 2, Bénédicte Lenoir 4, Nektarios A. Valous 4, Dirk Jäger 4,5, Emrullah Birgin 2, Tejas A. Sawant 1, Qi Li 6, Keshu Xu 7, Lingyue Dong 8, Timo Itzel 9,10, Andreas Teufel 9,10, Norbert Gretz 11, Lukas J.A.C. Hawinkels 12, Aránzazu Sánchez 13, Blanca Herrera 13, Rudolf Schubert 14, Han Moshage 15, Christoph Reissfelder 2,10, Matthias P. A. Ebert 1,10, Nuh Rahbari 2, and Katja Breitkopf-Heinlein 2.*submitted.

(6) *Identification of liver-derived bone morphogenetic protein (BMP)-9 as a potential new candidate for treatment of colorectal cancer.***Cai C**, Itzel T, Gaitantzi H, de la Torre C, Birgin E, Betge J, Gretz N, Teufel A, Rahbari NN, Ebert MP, Breitkopf-Heinlein K. J Cell Mol Med. 2022;26(2):343-353. PMID: 34841646.

(5) *BMP-9 modulates the hepatic responses to LPS.* Haristi Gaitantzi, Julius Karch, Lena Germann, **Chen Cai**, Vanessa Rausch, Emrullah Birgin, Nuh Rahbari, Courtney König, Hellmut Augustin, Carolina de la Torre, Norbert Gretz, Timo Itzel, Andreas Teufel, Matthias P. A. Ebert, Katja Breitkopf-Heinlein. Cells.2020 Mar 4;9(3):617.

(4) *Downregulation of SPARC Is Associated with Epithelial-Mesenchymal Transition and Low Differentiation State of Biliary Tract Cancer Cells.* Aghamaliyev U, Gaitantzi H, Thomas M, Simon-Keller K, Gaiser T, Marx A, Yagublu V, Araos C, **Cai C**, Valous NA, Halama N, Kiesslich T, Ebert M, Grützmann R, Rückert F, Breitkopf-Heinlein K. Eur Surg Res.2019;60(1-2):1-12. doi: 10.1159/000494734. Epub 2019 Jan 16.

(3) *Di (2-Ethylhexyl) Phthalate and Its Role in Developing Cholestasis: An In Vitro Study on Different Liver Cell Types.* Gaitantzi H, Hakenberg P, Theobald J, Heinlein C, **Cai C**, Loff S, Wölfl S, Ebert MP, Breitkopf- Heinlein K, Subotic U. J Pediatr Gastroenterol Nutr.2018 Feb;66(2):e28-e35.

(2) *BMP-9 interferes with liver regeneration and promotes liver fibrosis.* Breitkopf-Heinlein K, Meyer C, König C, Gaitantzi H, Addante A, Thomas M, Wiercinska C, **Cai C**, Li Qi, Wan F, Hellerbrand C, Valous NA, Hahnel M, Ehlting C, Bode JG, Müller-Bohl S, Klingmüller U, Altenöder J, Ilkavets I, Goumans MJ, Hawinkels LJ, Lee SJ, Wieland M, Mogler C, Ebert MP, Herrera B, Augustin H, Sánchez A, Dooley S, Ten Dijke P. Gut.2017 May;66(5):939-954. doi: 10.1136/gutjnl-2016-313314. Epub 2017 Mar 23.

(1) *The Wnt/β-catenin pathway regulates self-renewal of cancer stem-like cells in human gastric cancer.* **Chen Cai**, Xiaohan Zhu. Mol Med Rep. 2012 May;5(5):1191-1196.

12. Supplementary

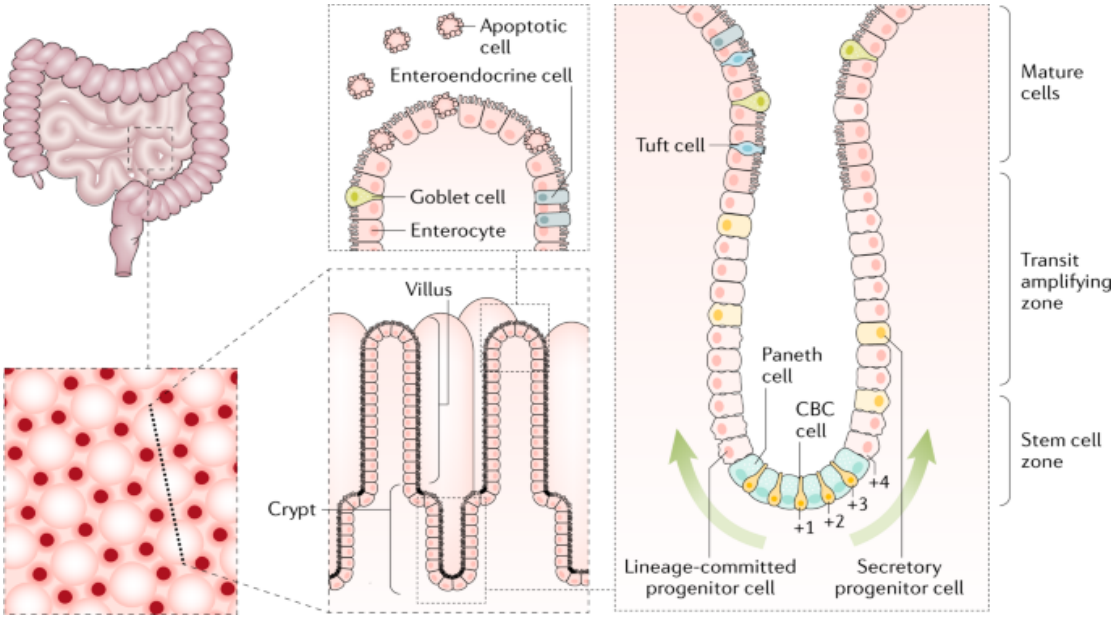

Suppl. Fig. 1: Intestinal crypts and villi. The intestinal epithelium are made of crypts and villi. At the bottom of crypts are stem cells. Stem cells own self-renew function to keep the stem cell number. At the same time, they can differentiate and migrate upwards toward the villus. The differentiated lineage-committed progenitor cells move into the transit amplifying zone, which then rapidly divide themselves. Villi are made of mature epithelial cells like absorptive enterocytes, goblet cells, enteroendocrine cells. Mature cells move towards the villus tip and apoptosis there.

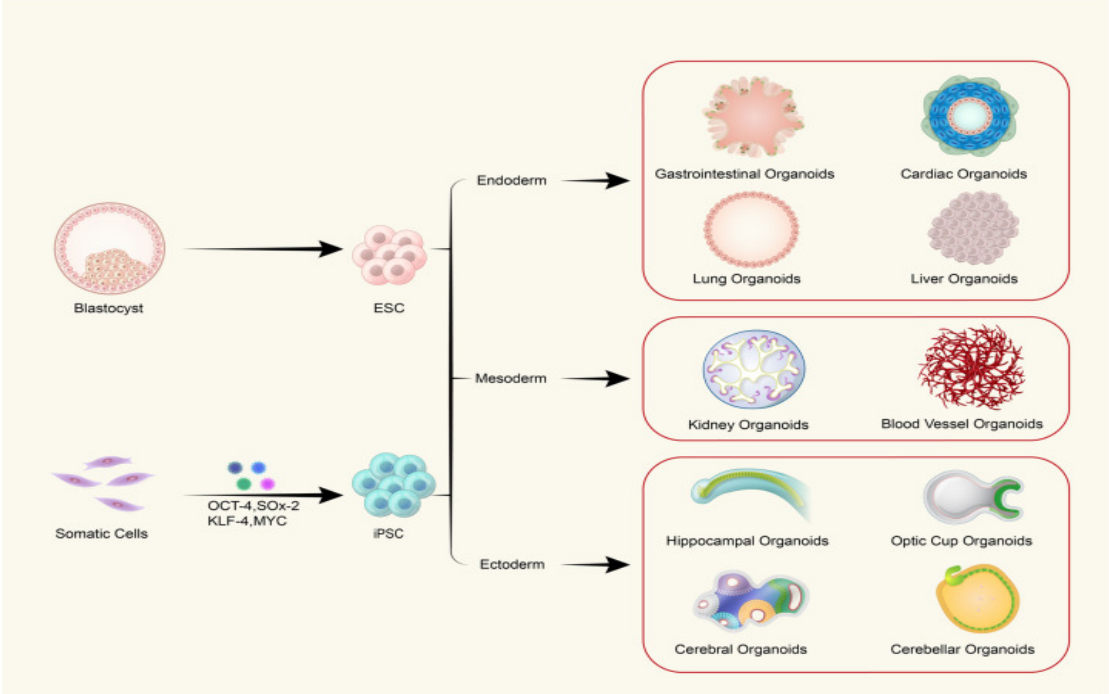

Suppl. Fig. 2: Schematic presentation of organoids isolation. Various organoids can be generated from either Embryonic stem cells (ESCs) or induced pluripotent stem cells (iPSCs)[50].

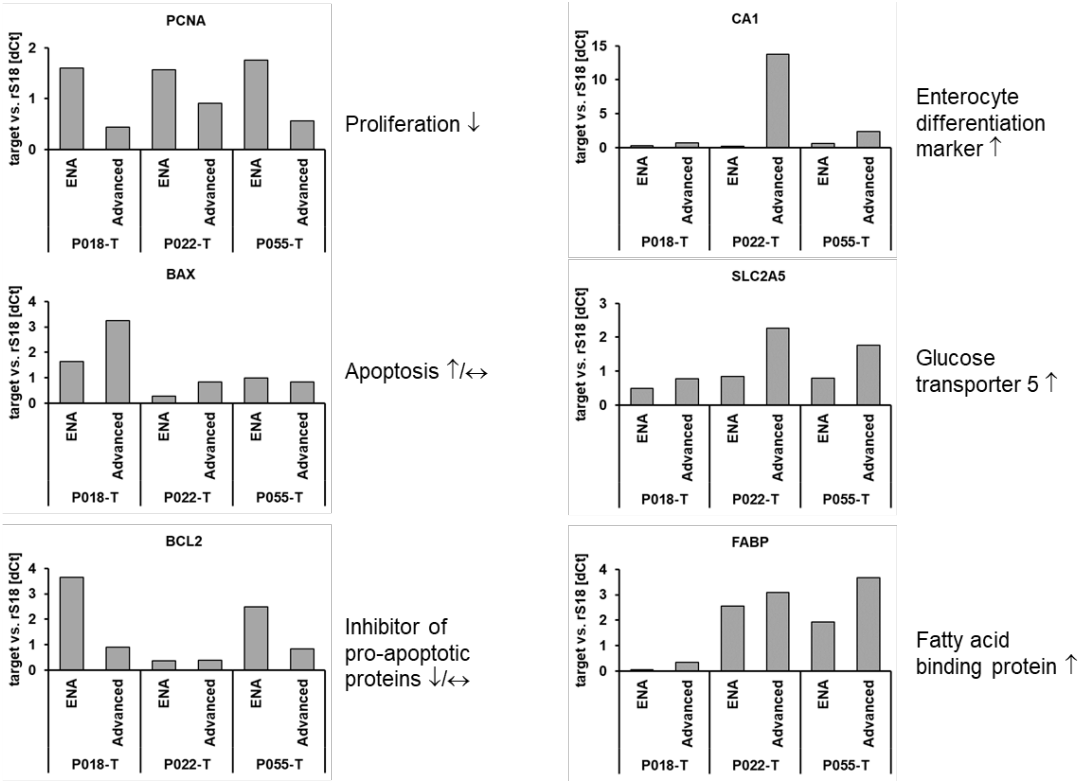

Suppl. Fig. 3: RT-PCR of colorectal tumour Organoids cultured in different medium. Tumour Organoids from 3 patients were either cultured in ENA or in advanced medium for 72 hours. RT-PCRs against general viability markers as well as markers of epithelial functionality were performed.

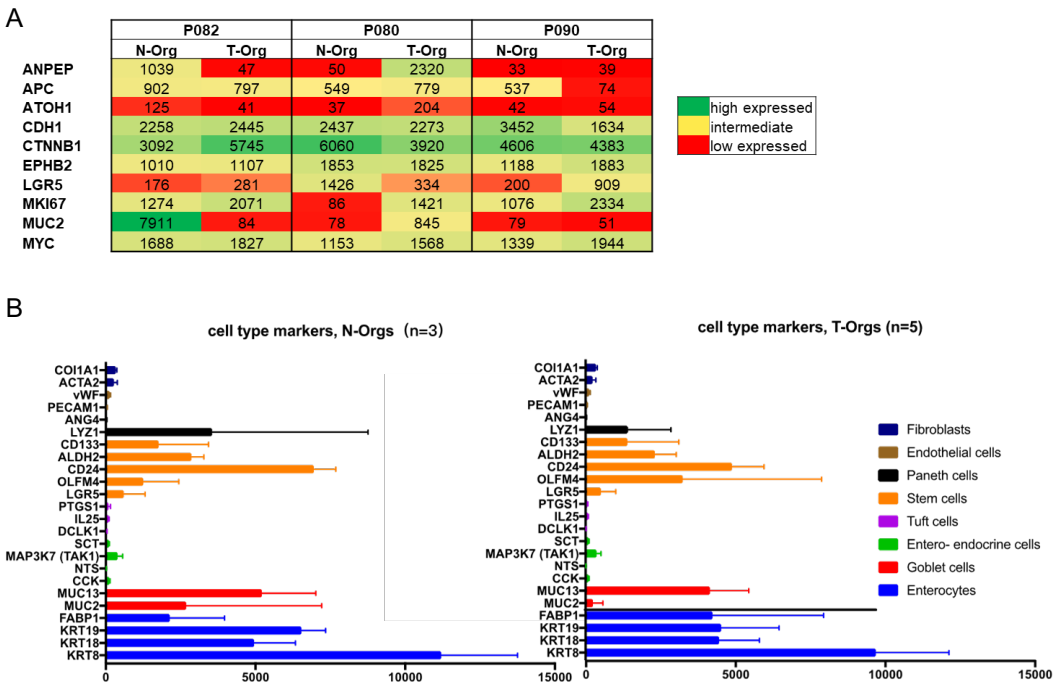

Suppl. Fig. 4: Expression levels of differentiation- and cell-type-markers in Tumor and Normal Organoids (T-Orgs and N-Orgs, respectively). A) Individual expression levels of a set of classical differentiation-marker genes. Numbers given are the unlogged values obtained by Affymetrix array analyses. B) Expression levels of the cell-type markers of the indicated cell types expressed in both N- and T-Orgs. Numbers on the X-axis are the average values of patients P082, P080 and P090 for N-Orgs and of patients P018, P055, P082, P080 and P090 for T-Orgs (unlogged data) +/- SEM obtained by Affymetrix array analyses.

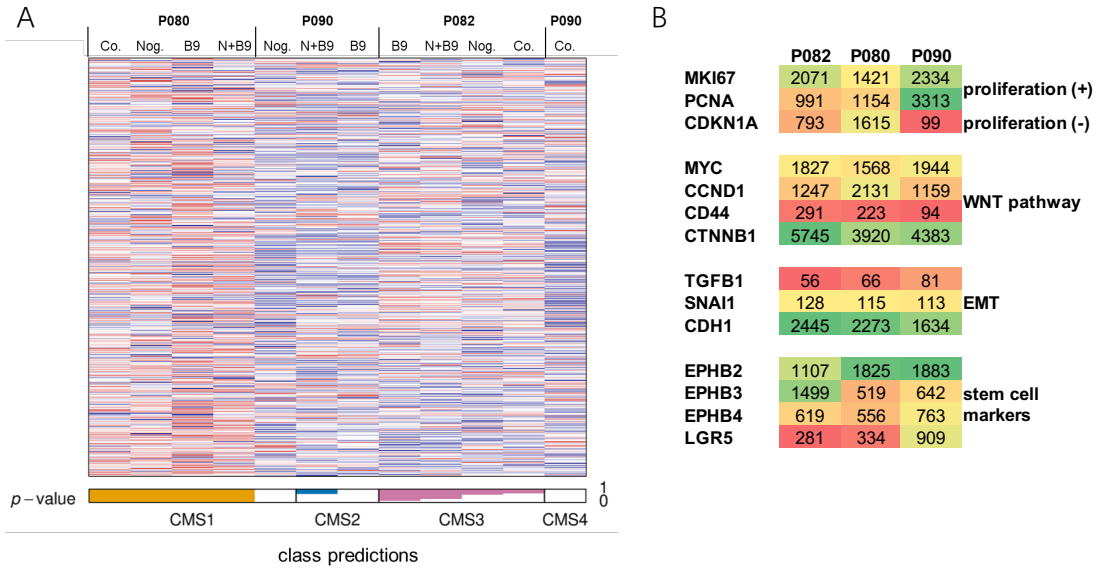

Suppl. Fig. 5: Analysis of the consensus molecular subtypes (CMS) of organoids from patients 082, 080 and 090. A) Analysis of the expression profiles of T-Orgs from all 3 patients (Co: untreated; Nog: Noggin-treated; B9: BMP-9-treated; N+B9: treated with both, BMP-9 and Noggin simultaneously). "CMScaller", an R package that was established in order to define the CMS of samples from colorectal cancer pre-clinical models, like organoids, based on expression profiles was used[60]. With an input of only 12 samples many p-values did not reach statistical significance (white areas in the p-value bar at the bottom). Nevertheless, the results imply that P080 belongs to CMS1, P082 to CMS3 and P090 either to CMS2 or 4. B) Heat-map showing the expression levels (unlogged values taken from affymetrix array results) of selections of marker genes for the indicated groups in T-Orgs of the 3 patients. Proliferation (+): pro-proliferative genes; Proliferation (-): anti-proliferative gene.

	P018-T	P055-T	P080-T	P082-T	P090-T
Method	Amplicon Seq	Amplicon Seq	Exome Seq	NA	Exome Seq
Mutated genes	None identified	NRAS	SLC25A24 TRAK1 CSMD1 ANKRD2 KRAS DZIP1 YTHDF1	NA	OR10J1 **APC** FZD6 APBA1 **TP53** SEZ6L

RNA-level	P018-T	P055-T	P080-T	P082-T	P090-T
APC	342	312	691	797	74
TP53	1112	978	1543	714	191

Suppl. Fig. 6: Analysis of the mutation status of the tumours. Amplicon or exome sequencing of DNA from T-Orgs was performed as indicated in the upper table. The lower table shows the corresponding expression levels of APC and p53 as determined in the array analyses. NA: not analyzed. The results indicate that P090 harbours APC as well as TP53 mutations that result in strongly reduced expression levels of both genes.

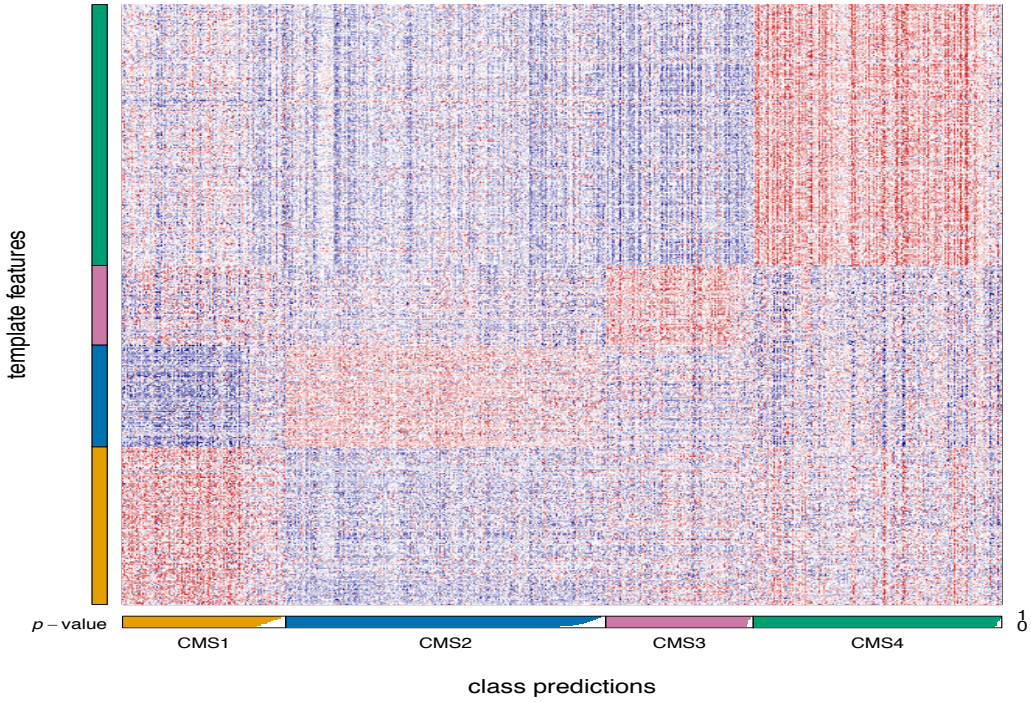

Suppl. Fig. 7: Analysis of the CMS subgroup of TP53 mutated patient's data Online data GSE39582 was analysed by R package "CMScallerR and shows that TP53 mutated CRC patients samples mainly belongs to CMS 2(48.82%) and 4(31.18%).

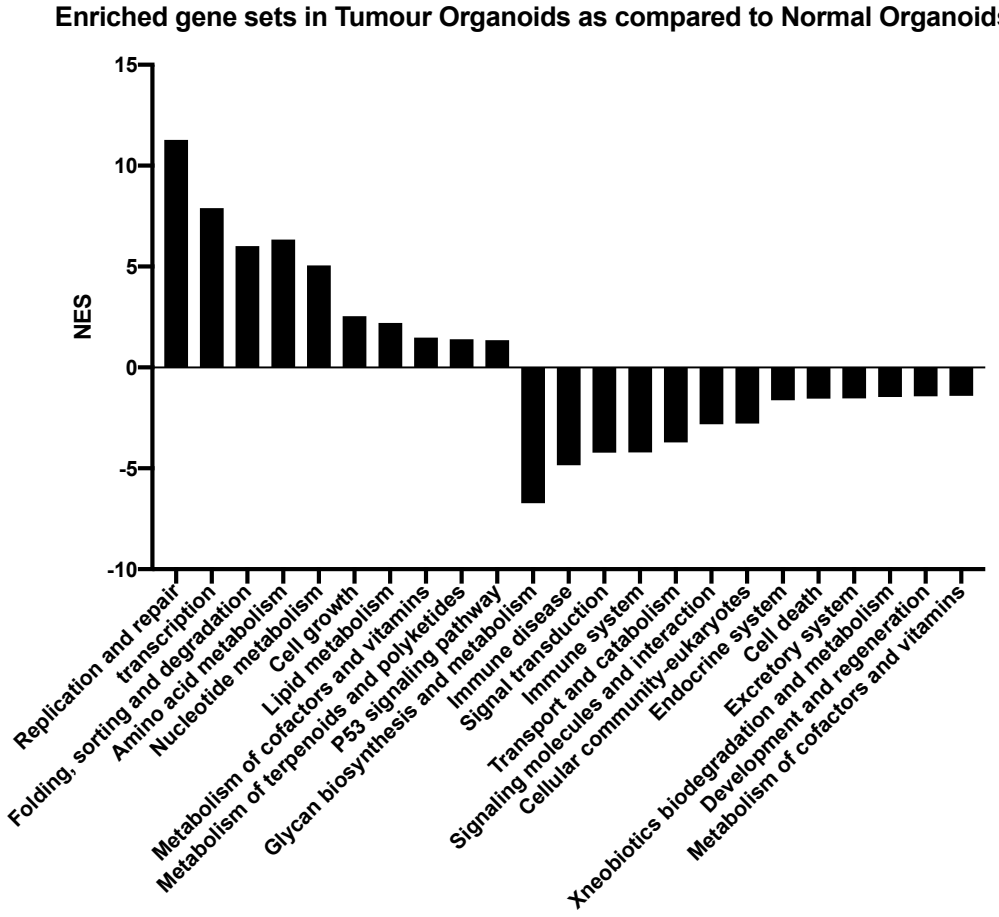

Suppl. Fig. 8: Enriched gene sets in T-Orgs compared to N-Orgs of all 3 patients. Gene sets enrichment analysis (GSEA) was performed focusing on the Kyoto Encyclopedia of Genes and Genomes (KEGG). A false discovery rate (FDR) lower than 0.25 and a p-value lower than 0.05 was considered as statistically significant. NES: normalized enrichment score.

A

top 30 down-regulated genes

	sorted by patient 080			sorted by patient 082			sorted by patient 090		
		P080	P082	P090	P080	P082	P090	P080	P082	P090
	Gene Symbol	fold change			fold change			fold change		
1	MT2A	-6,55	-0,26	0,58	CA1	0,59	-8,25	0,81	HMGCS2	-0,67	1,02	-5,60
2	MT1F	-5,11	-0,82	0,75	CLCA4	-0,23	-7,11	-0,80	ID1	2,12	3,49	-5,59
3	MAP1B	-5,02	-0,25	-0,53	MMP7	3,70	-6,92	-0,70	CXCL5	-0,09	5,00	-5,52
4	KRT39	-4,88	0,32	0,48	REG4	4,53	-6,90	0,30	FABP1	5,51	-1,09	-5,43
5	OR51E1	-4,74	0,07	-0,30	TCN1	0,10	-6,39	-0,10	LCP1	-0,10	5,86	-5,08
6	GABRA3	-4,60	-0,26	-0,17	CTSE	4,96	-6,19	-1,80	TREML2	-2,56	2,70	-4,81
7	TMEM150C	-4,39	2,43	-0,23	MUC2	2,53	-6,08	-0,23	ADGRG7	-3,18	0,10	-4,63
8	MT1E	-4,31	-3,03	-0,42	PIGR	6,85	-6,06	-0,89	FRMD3	1,35	-0,64	-4,56
9	NRCAM	-4,21	0,44	4,25	CA2	0,69	-5,60	-0,38	ST3GAL4	0,34	-1,98	-4,48
10	TNFRSF10C	-4,19	-3,73	-0,14	PLAC8	0,64	-5,36	0,18	TDRD1	0,65	4,04	-4,33
11	NFE2	-4,18	2,37	-1,26	SI	0,15	-5,20	-0,53	DMKN	0,73	-0,99	-4,30
12	RHOBTB1	-4,16	0,11	-0,38	RARRES1	0,44	-5,18	0,92	OAS1	0,88	2,04	-4,20
13	SCD5	-4,16	-1,48	2,62	F3	0,62	-5,09	-0,32	PLOD2	0,07	0,69	-4,12
14	RGCC	-4,13	0,86	0,76	LYZ	0,34	-5,07	-0,92	C10orf99	0,36	1,10	-4,09
15	ABHD12B	-4,06	1,36	0,08	NTRK2	0,24	-5,04	0,37	CEACAM5	5,11	-0,54	-3,99
16	PCDH19	-4,01	-0,30	5,44	EVI2B	0,86	-5,03	0,76	PGC	1,85	3,42	-3,97
17	MT1B	-3,96	-0,67	-0,42	GCNT3	3,74	-5,02	-2,05	FXYD3	1,48	-1,72	-3,84
18	IGF2BP1	-3,95	-0,25	0,41	SLC38A5	-0,54	-4,97	5,24	SLCO1B3	-0,98	-2,22	-3,82
19	ROBO1	-3,90	0,91	-2,07	EPB41L4A	0,72	-4,86	-1,00	CDKN1A	1,21	-0,68	-3,82
20	NRXN3	-3,83	2,49	1,78	SLC6A14	1,27	-4,86	-1,36	ID3	3,42	2,91	-3,81
21	PROM1	-3,67	-3,88	5,58	DHRS9	2,08	-4,80	-0,29	IFI27	3,10	-1,46	-3,75
22	CADM1	-3,66	0,29	1,49	SLC4A4	-0,29	-4,78	0,82	LGALS1	2,15	2,54	-3,74
23	PHLDB2	-3,64	-0,12	-1,11	FAM198B	1,93	-4,78	-1,03	S100A4	2,90	1,77	-3,73
24	MT1A	-3,55	-0,23	0,31	CLCA1	0,42	-4,73	0,05	DAB2	1,44	-1,32	-3,72
25	TLE4	-3,50	-0,39	-1,21	IGFBP3	-0,08	-4,72	0,92	CYP2B6	-0,28	2,96	-3,63
26	MRPS21	-3,48	-0,44	0,17	SPON1	-0,21	-4,68	0,33	CDA	2,00	0,78	-3,60
27	FAM3B	-3,43	5,29	-1,73	AGR3	2,49	-4,53	0,66	PADI3	0,71	1,27	-3,59
28	TMEM200A	-3,37	-0,89	1,40	PADI2	2,50	-4,39	-0,49	COL17A1	1,02	-3,04	-3,57
29	DMD	-3,25	-0,02	2,61	FER1L6	2,26	-4,38	0,00	FER	0,42	1,57	-3,56
30	MEF2C	-3,22	-4,22	0,05	LYPD8	-0,67	-4,36	1,25	KRT20	1,62	-0,96	-3,52

B

top 30 up-regulated genes

	sorted by patient 080			sorted by patient 082			sorted by patient 090		
		P080	P082	P090	P080	P082	P090	P080	P082	P090
	Gene Symbol	fold change			fold change			fold change		
30	CDK1	3,79	1,38	0,26	FABP6	1,56	3,21	-1,85	PRNP	0,21	-2,05	2,88
29	CCNA2	3,88	0,01	1,77	PTCH1	-0,96	3,28	-2,99	SLC6A20	1,91	-1,67	2,89
28	TOP2A	3,90	1,56	1,27	NCAM1	-0,04	3,31	-2,81	GNPDA2	0,21	-1,97	2,92
27	ARHGAP11A	3,92	1,49	1,28	RUBCNL	-1,88	3,32	0,07	SLFN13	1,53	-0,83	3,00
26	RRM2	3,92	1,06	1,19	GNG4	-1,43	3,39	0,83	RNF182	-0,23	-0,32	3,06
25	ATOH1	3,94	-2,17	0,36	PGC	1,85	3,42	-3,97	CLDN2	-1,90	-1,46	3,09
24	DPP4	4,02	-1,67	-2,41	KRT23	-1,48	3,45	-0,19	OXCT1	1,83	-1,13	3,20
23	CEACAM7	4,02	-3,63	-1,79	ID1	2,12	3,49	-5,59	DRD2	-0,45	0,56	3,25
22	PCLAF	4,09	1,19	1,62	CRNDE	0,30	3,50	1,43	ZNF22	-0,42	-0,75	3,36
21	DLGAP5	4,19	0,43	1,10	MAN1A1	-0,49	3,51	0,64	GSTM3	1,52	-3,91	3,41
20	ACAT2	4,22	0,82	0,39	FBXO27	-1,10	3,56	-1,49	DPP10	-0,12	-0,55	3,47
19	TSPAN7	4,27	-0,12	0,09	GLIPR1	-0,54	3,59	-1,79	SLAMF6	0,40	0,41	3,48
18	FADS2	4,31	-3,48	-1,58	HUNK	-0,30	3,60	0,51	NECTIN3	-0,17	-1,60	3,53
17	AKR1B10	4,38	-2,87	-1,44	EYA1	-0,02	3,63	-1,98	C3orf14	2,70	-0,60	3,58
16	IL33	4,42	0,92	-3,20	LRP4	-2,40	3,76	0,80	PTPRO	3,62	4,72	3,59
15	EREG	4,45	1,42	0,87	IFITM1	-1,04	3,76	-3,37	GABRB2	-0,35	0,22	3,73
14	REG4	4,53	-6,90	0,30	PTPRD	-1,17	3,79	1,15	REG1A	1,17	-0,10	3,87
13	SRPX	4,53	0,12	1,09	BCL11A	-1,17	3,99	1,03	SPTLC3	-0,67	-1,68	4,13
12	SYTL5	4,53	-1,39	0,01	KRT75	-0,25	4,04	-2,88	CPA2	-2,39	0,36	4,14
11	SLC9A2	4,64	-0,30	-2,21	TDRD1	0,65	4,04	-4,33	ZNF286A	1,46	-3,25	4,14
10	SERPINA1	4,89	-0,10	-1,53	PAH	0,42	4,10	-1,69	NRCAM	-4,21	0,44	4,25
9	CEACAM6	4,93	0,44	-3,38	APCDD1	-1,88	4,12	-1,17	CST7	-2,55	0,06	4,34
8	C1orf21	4,96	-1,33	1,86	AGMO	-0,52	4,34	-3,06	HEXA	-0,20	-3,11	4,36
7	CTSE	4,96	-6,19	-1,80	DACH1	-1,29	4,47	1,85	CYP4X1	-2,35	-0,71	4,50
6	IL2RG	4,96	-1,34	-0,62	PROX1	-0,83	4,50	1,00	SLC38A5	-0,54	-4,97	5,24
5	TRIM31	4,96	-1,66	-3,05	PTPRO	3,62	4,72	3,59	ANOS1	0,35	-0,45	5,24
4	ANPEP	5,06	-4,21	0,11	CXCL5	-0,09	5,00	-5,52	UCHL1	0,39	-1,95	5,37
3	CEACAM5	5,11	-0,54	-3,99	FAM3B	-3,43	5,29	-1,73	PCDH19	-4,01	-0,30	5,44
2	FABP1	5,51	-1,09	-5,43	LCP1	-0,10	5,86	-5,08	PROM1	-3,67	-3,88	5,58
1	PIGR	6,85	-6,06	-0,89	PCP4	-2,91	6,40	-0,71	OLFM4	0,22	1,58	6,22
43	PTPRO	3,62	4,72	3,59								

Suppl. Fig. 9: Individual expression changes in T-Orgs compared to corresponding N-Orgs. Genes down-regulated (A) and up-regulated (B) in T-Orgs vs. N-Orgs of the three patients (P080, P082 and P090).

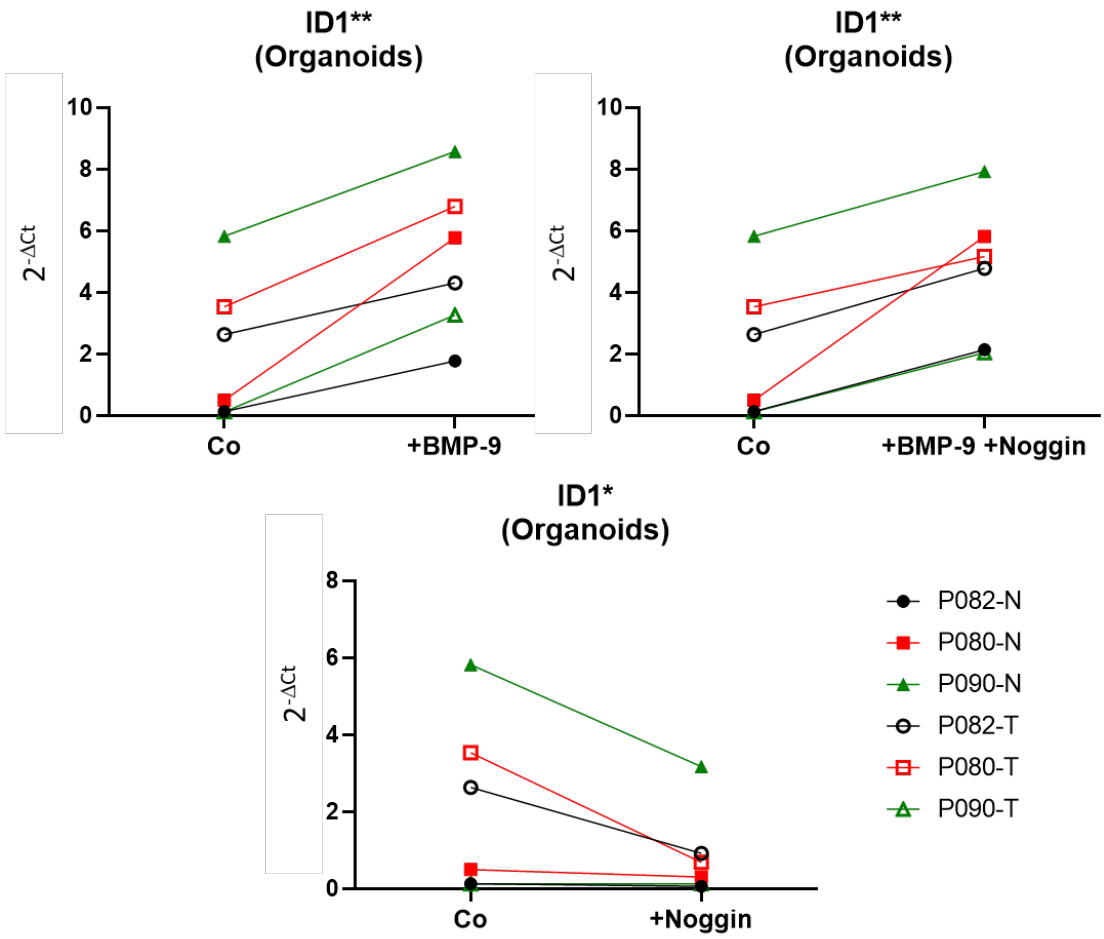

Suppl. Fig. 10: Noggin reduces and BMP-9 enhances ID1 expression in Organoids. As validation of the array data shown in Fig. 13A real-time PCR was performed using the same samples. Organoids were derived from human biopsies of normal and cancerous gut mucosa as depicted in fig.5 followed by in vitro stimulation with either recombinant Noggin (100 ng/ml) or BMP-9 (5 ng/ml) or both together. After 48 h RNA was isolated and processed for real-time PCR analyses. The scores (normalized to the house-keeping gene rS18) for the individual ID1 expression in each sample (N as well as T of each patient's organoids) are plotted and values of untreated (Co.) are compared to either BMP-9-treated (+BMP-9), Noggin-treated (+Noggin) or treated with both (+BMP-9 +Noggin). For statistics all 6 controls were compared to all 6 treated samples and significance was calculated using the paired t-test. *=p>0.05; **=p>0.01.

	P018		P055		P080			
	basal	co-culture	basal	co-culture	basal	co-culture	logFC	P.Value
BMPR1A	9,76	9,61	9,63	10,11	9,66	9,36	0,01	0,9734
BMPR1B	5,47	4,95	5,23	5,41	5,04	4,30	-0,36	0,2285
ACVR1 (=Alk2)	8,31	8,63	8,57	8,62	8,97	8,64	0,01	0,9663
ACVRL1 (=Alk1)	7,81	7,78	8,22	8,26	7,08	7,37	0,10	0,7480
ACTR1A	9,96	10,06	10,08	10,11	10,26	10,15	0,00	0,9928
ACTR1B	8,89	8,87	9,13	8,76	8,89	8,97	-0,10	0,5335
BMPR2	9,73	9,64	9,57	9,83	9,57	9,57	0,05	0,7102
ACVR2A	7,83	7,93	8,27	8,22	7,02	7,18	0,07	0,8394
ACVR2B	5,55	6,00	5,43	5,86	6,10	5,40	0,06	0,8420

higher expressed
no change
lower expressed

Suppl. fig. 11: BMP-receptor expression is not significantly changed in CAFs by co-culture with T-Orgs. Basal as well as co-culture-mediated expression of BMP-type I and type II receptors was determined in CAFs. Expression levels that were enhanced by co-culture are shown in green, those reduced in red and unchanged in yellow. logFC: average fold change (log data) of all three patients.

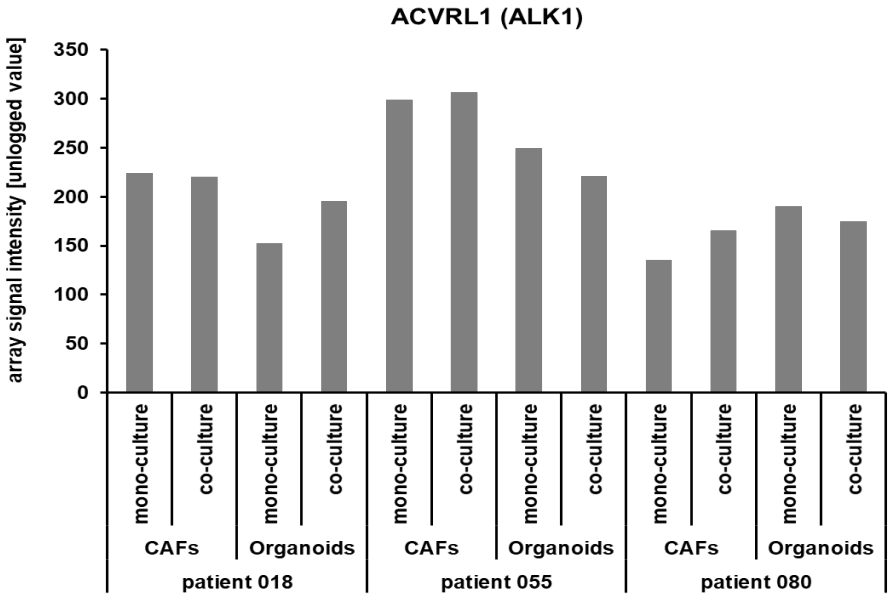

Suppl. Fig 12: Expression of Alk1 is mainly unchanged by co-culture in CAFs as well as T-Orgs. The expression levels for Alk1(ACVRL1) are shown in all samples in direct comparison.

13. Tables

	NCCN	USPSTF	ACS/USMSTFIACR	ACG
Detect cancer				
guaiac Fecal Occult Blood Test (gFOBT)	Annual	Annual	Annual	Annual
Fecal Immunochemical Test (FIT)	Annual	Annual	Annual	Annual
Stool DNA (FIT-DNA)	Every 3 years	Every 1 or 3 years	Every 3 years	Interval uncertain
Detect cancer and polyps				
Flexible Sigmoidoscopy	Every 5-10 years +/- gFOBT/FIT every 3 years	Every 5 years OR Every 10 years + annual FIT	Every 5 years +/- annual gFOBT/FIT	Every 5 years
Colonoscopy	Every 10 years	Every 10 years	Every 10 years	Every 10 years
Computed Tomography Colonography (CTC)	---	---	Every 5 years	Every 5 years
Barium enema	---	---	Every 5 years	Every 5 years

Table 1: Summary of colorectal cancer screening guidelines. Abbreviations: NCCN: National Comprehensive Cancer Network. ACS: American Cancer Society.USMSTF: U.S.

Multi-Society Task Force.ACR: American College of Radiology.USPSTF: U.S. Preventive Services Task Force.ACG: American College of Gastroenterology[5].

Patient ID	**Gender**	**Age at time of biopsy (in years)**	**Tumour staging**	**Type of tumour**
P080	f	65	T3, N1, M0	rectum adenocarcinoma
P082	f	49	T3, N1, M0	rectum adenocarcinoma
P090	m	74	T3, N0, metachronous hepatic and pulmonal metastases	sigmoid adenocarcinoma

Table 2: Patient details.

WENRA	**final concentration**
Wnt3a	conditioned medium, 50%
R-Spondin	conditioned medium, 20%
Noggin	conditioned medium, 10%
B27	1:50
Nicotinamid	10 mM
NAC	1.25 mM
Primocin	100 mg/ml
EGF	50 ng/ml
Y-27632	10 µM
A83-01	500 nM
PGE2	10 nM
Gastrin	10 nM

Table 3: List of media components. For initiation of organoid formation and for amplification of generated organoid lines ENA and WENRAS media, containing many growth factors, inhibitors and other components as listed above, were used. ENA is equal to WENRA except that no Wnt3a or R-Spondin is added. All components were combined in basal medium (=Advanced DMEM/F12). Conditioned medium was produced as previously described[87]. To avoid interferences with the BMP-pathway by any of these components, the medium was always changed to a basal medium, comprised of only Advanced DMEM/F12 during the actual BMP-9/noggin stimulations or CAFs-organoids co-culture.

Target gene	**Forward sequence**	**Reverse sequence**
hACVRL1	CATCGCCTCAGACATGACCTC	GTTTGCCCTGTGTACCGAAGA
hID1	GTTTCAGCCAGTCGCCAGA	CAGCCGTTCATGTCGTAGAGCA
h+mRS18	CCATTCGAACGTCTGCCCTAT	TCACCCGTGGTCACCATG
mGDF2	CAGAACTGGGAACAAGCATCC	GCCGCTGAGGTTTAGGCTG
mACVRL1	GGCCTTTTGATGCTGTCG	ATGACCCCTGGCAGAATG
mID1	ATCCTGCAGCATGTAATCGAC	GCCTCAGCGACACAAGATG
mB2M	TTCTGGTGCTTGTCTCACTGA	CAGTATGTTCGGCTTCCCATTC

Table 4. Sequences of the primers used for real-time PCR (5' => 3' orientation). GDF2 = BMP-9, bone morphogenetic protein 9; ACVRL1 = ALK1, activin receptor-like kinase1; ID1 = inhibitor of DNA binding 1 HLH protein; RS18 = Ribosomal protein S18; B2M = Beta-2-Microglobulin; Primers targeting human GDF2 (BMP-9) were purchased from Qiagen (Germany): pre-designed sequence: QT00210462. *h* = human; *m* = mouse.

14. Curriculum Vitae

Name:	Chen Cai
Staatsangehörigkeit:	China
Geburtsdatum:	1986-03-10
Geschlecht:	Weiblich
E-Mail-Adresse:	chentsai925@yahoo.com
Berufserfahrung:	
2022-09-	Assistenzärztin Geriatrie am Universitätsklinikum Mannheim, Baden-Württemberg Deutschland
2012-08 - 2016-07:	Assistenzärztin Gastroenterologie am Zweiten Volkskrankenhaus von Changzhou, China.
Ausbildung:	
2016-12 – 2022-8:	*Promotion* Universitätsmedizin Mannheim
2012:	*Master Abschluss der Innere Medizin* Central South Universität, Hunan China.
2009:	*Bachelor Abschluss der Medizin* Tongji Medical College, Huazhong Universität für Wissenschaft und Technologie Wuhan China.

15. Acknowledgment

This project would not have been possible without the kind help of individuals and organizations. I would like to extend my sincere gratitude to all of them.

First and foremost, I have to thank my research supervisor PD Dr. rer. nat. Katja Breitkopf-Heinlein for her assistance and dedicated involvement in every step throughout the process. Her unrivaled scientific attitude and meticulous academic spirit inspired me deeply. I also appreciate a lot her guidance and support in my daily life.

Secondly, I am very grateful to express my sincere appreciation to Mr.Timo Itzel for his constant assistance and constructive advice in microarray data processing and database analyzing. I also would like to thank Mrs.Haristi Gaitantzi for her fully support in experimental skills and organizations. Mr. Christof Dormann did not only inspired me a lot in Basic Experimental Skills, but also sparked my interests in experimenting.

Then, I would like to express my sincere thanks to all the co-workers for their scientific and technical support: Mrs. Kauthar Srour, Mrs.Carolina de la Torre, Mr. Emrullah Birgin ,Mr. Joaquín Araos Henríquez, Mr. Johannes Betge , Pro. Norbert Gretz , Pro.Andreas Teufel , Pro. Nuh N Rahbari.

Words cannot express how grateful I am to Professor M.D. Matthias P. A. Ebert and my committee chair, for their invaluable patience and feedback. I also would not have been able to embark on this journey without my defense committee, who generously provided their knowledge and expertise. Furthermore, this endeavor would not have been possible without the generous support of the China Scholarship Council, which funded my research.

Lastly, I would like to thank my family. They are the home of my soul.